

Supporting Information

Exploring the catalytic and anticancer activity of gold(I) complexes bearing 1,3,5-traza-7-phosphaadamantane (PTA) and related ligands

Nuno Reis Conceição,*¹ Abdallah G. Mahmoud,^{2,3} Martin C. Dietl,⁴ Isabella Caligiuri,⁵ Flavio Rizzolio,^{5,6} Sónia A. C. Carabineiro,*^{1,2} Matthias Rudolph,⁴ M. Fátima C. Guedes da Silva,^{1,7} Armando J. L. Pombeiro,¹ A. Stephen K. Hashmi,⁴ and Thomas Scattolin*⁸

¹ Centro de Química Estrutural, Institute of Molecular Sciences, Instituto Superior Técnico, Universidade de Lisboa, Av. Rovisco Pais, 1049-001 Lisboa, Portugal

² LAQV-REQUIMTE, Department of Chemistry, NOVA School of Science and Technology, Universidade NOVA de Lisboa, 2829-516 Caparica, Portugal

³ Department of Chemistry, Faculty of Science, Helwan University, Ain Helwan, Cairo 11795, Egypt

⁴ Organisch-Chemisches Institut, Heidelberg University, Im Neuenheimer Feld 270, 69120 Heidelberg, Germany

⁵ Pathology Unit, Department of Molecular Biology and Translational Research, Centro di Riferimento Oncologico di Aviano (CRO) IRCCS, via Franco Gallini 2, 33081, Aviano, Italy

⁶ Dipartimento di Scienze Molecolari e Nanosistemi, Università Ca' Foscari, Campus Scientifico Via Torino 155, 30174 Venezia-Mestre, Italy

⁷ Departamento de Engenharia Química, Instituto Superior Técnico, Universidade de Lisboa, Av. Rovisco Pais, 1049-001 Lisboa, Portugal

⁸ Dipartimento di Scienze Chimiche, Università degli studi di Padova, via Marzolo 1, 35131, Padova, Italy

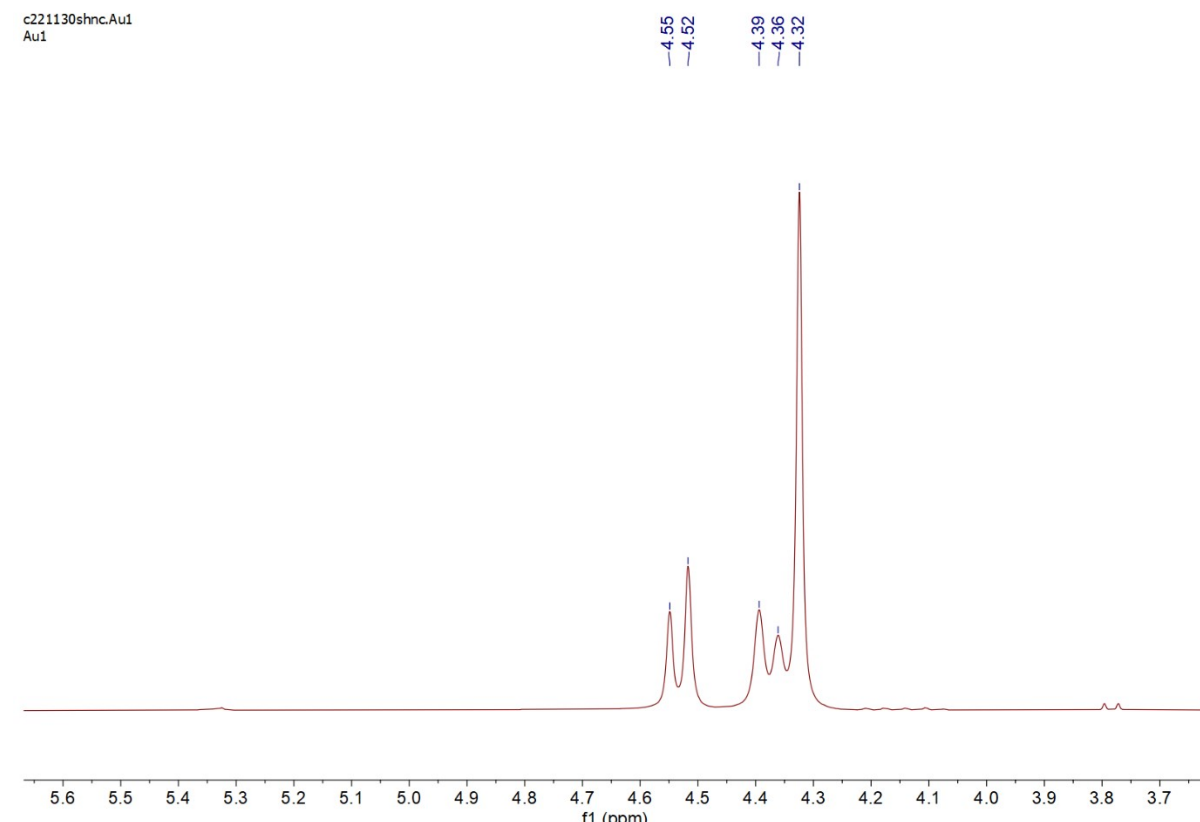


Figure S1. ¹H NMR spectrum of compound 1 collected in (CD₃)₂SO (400 MHz).

c221130shnc.Au1
Au1

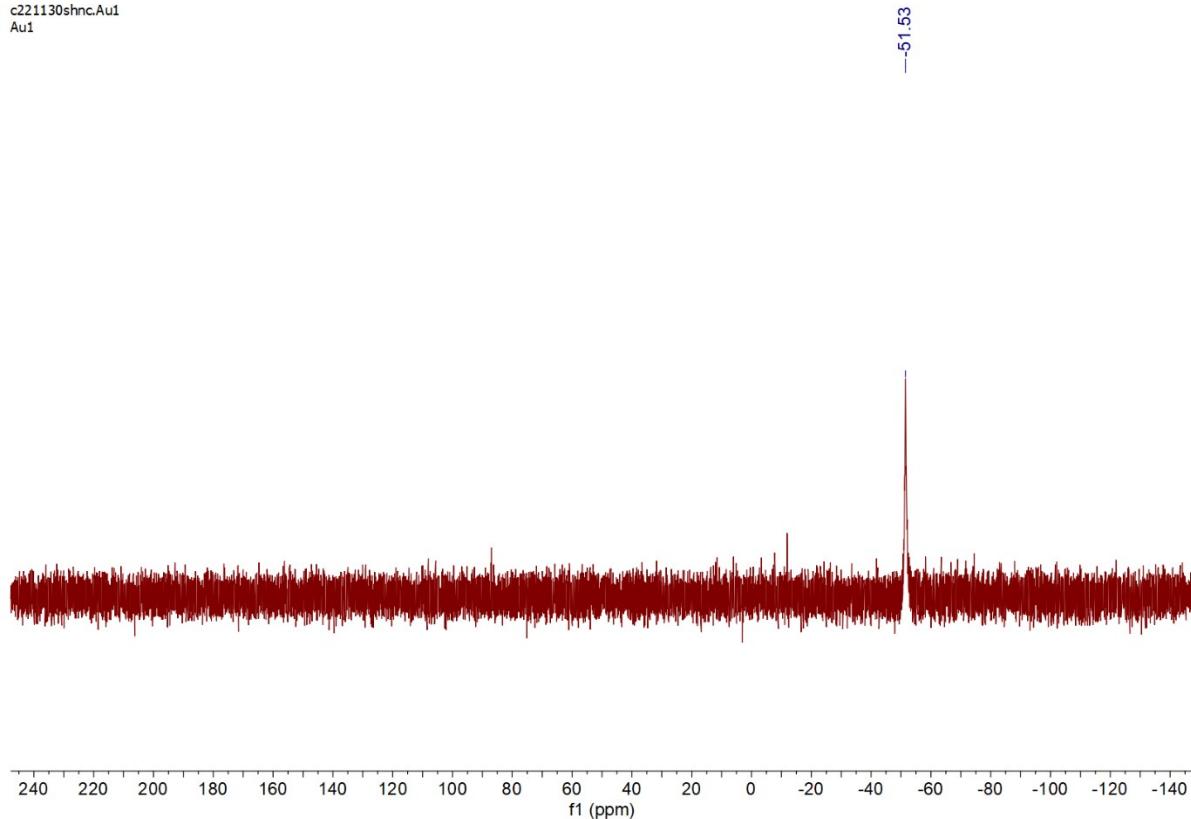


Figure S2. ^{31}P NMR spectrum of compound **1** collected in $(\text{CD}_3)_2\text{SO}$ (400 MHz).

c221212shnc.Au1s2

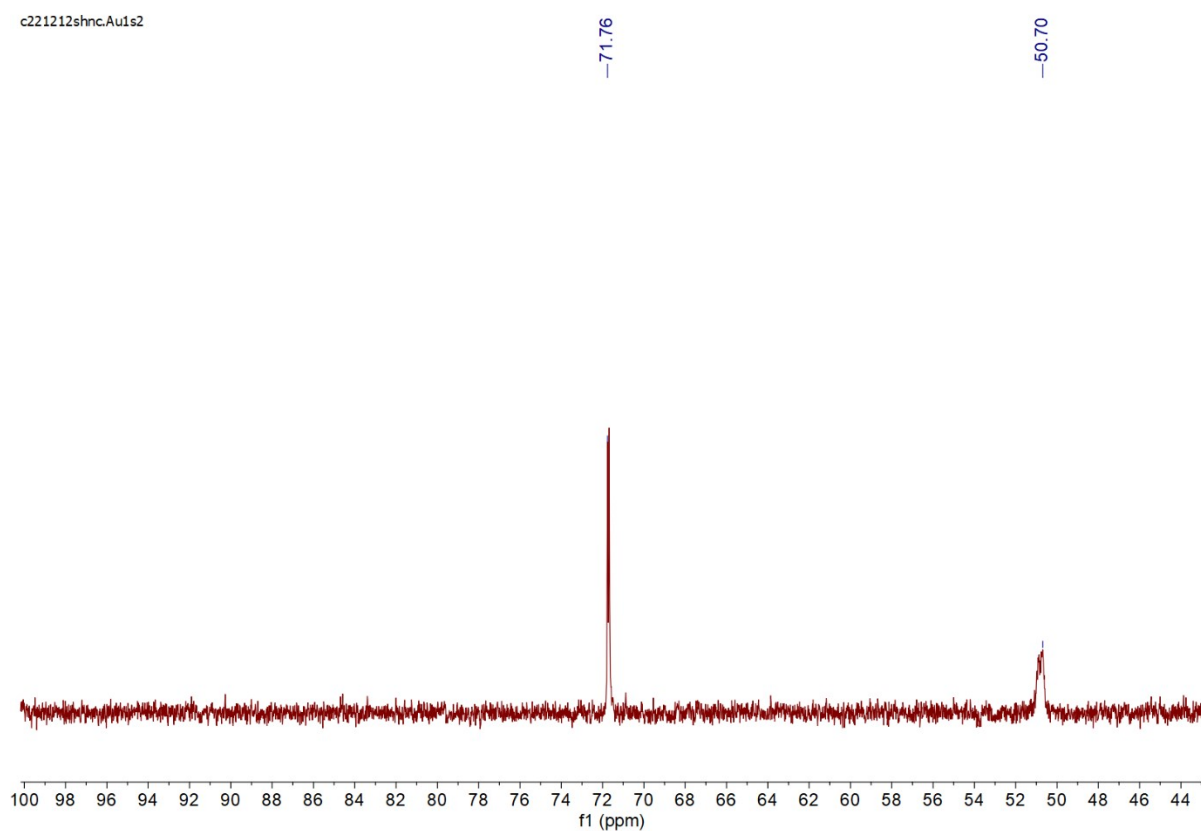


Figure S3. ^{13}C NMR spectrum of compound **1** collected in $(\text{CD}_3)_2\text{SO}$ (400 MHz).

c221212shnc.Au1s2

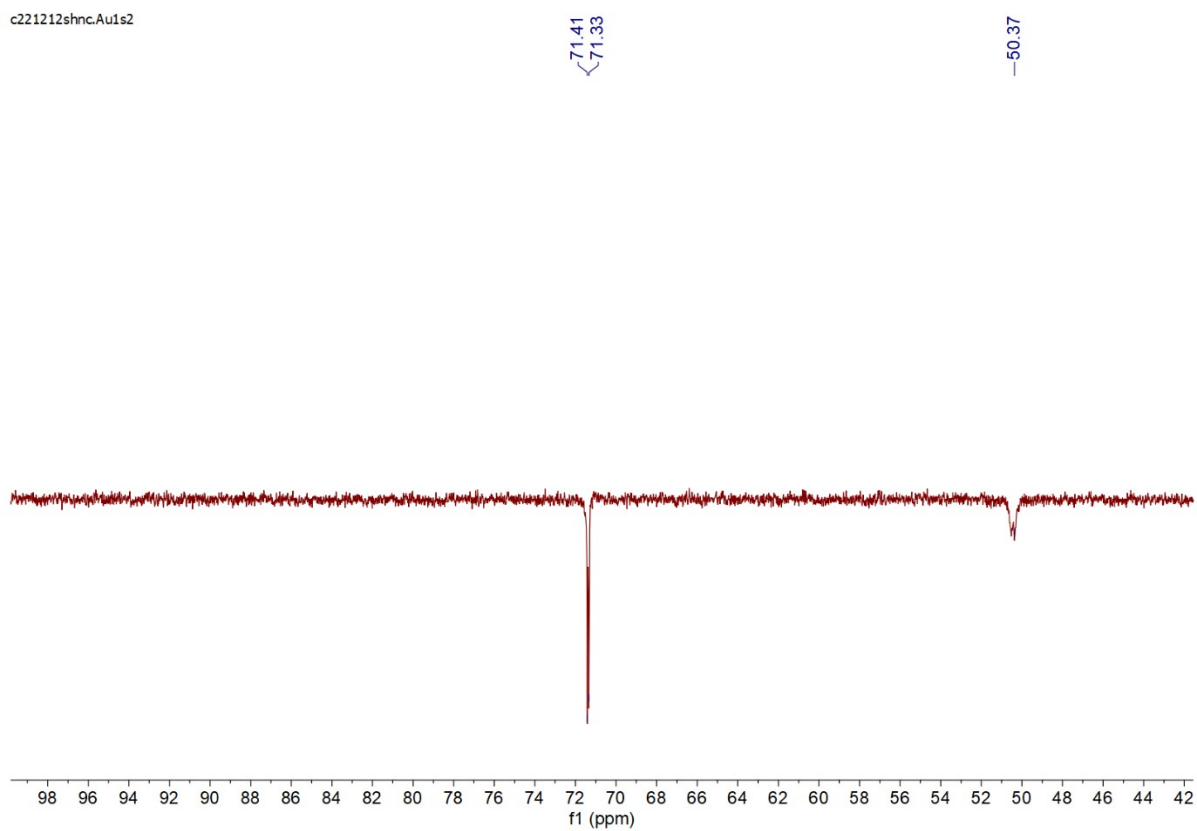


Figure S4. DEPT NMR spectrum of compound **1** collected in $(CD_3)_2SO$ (400 MHz).

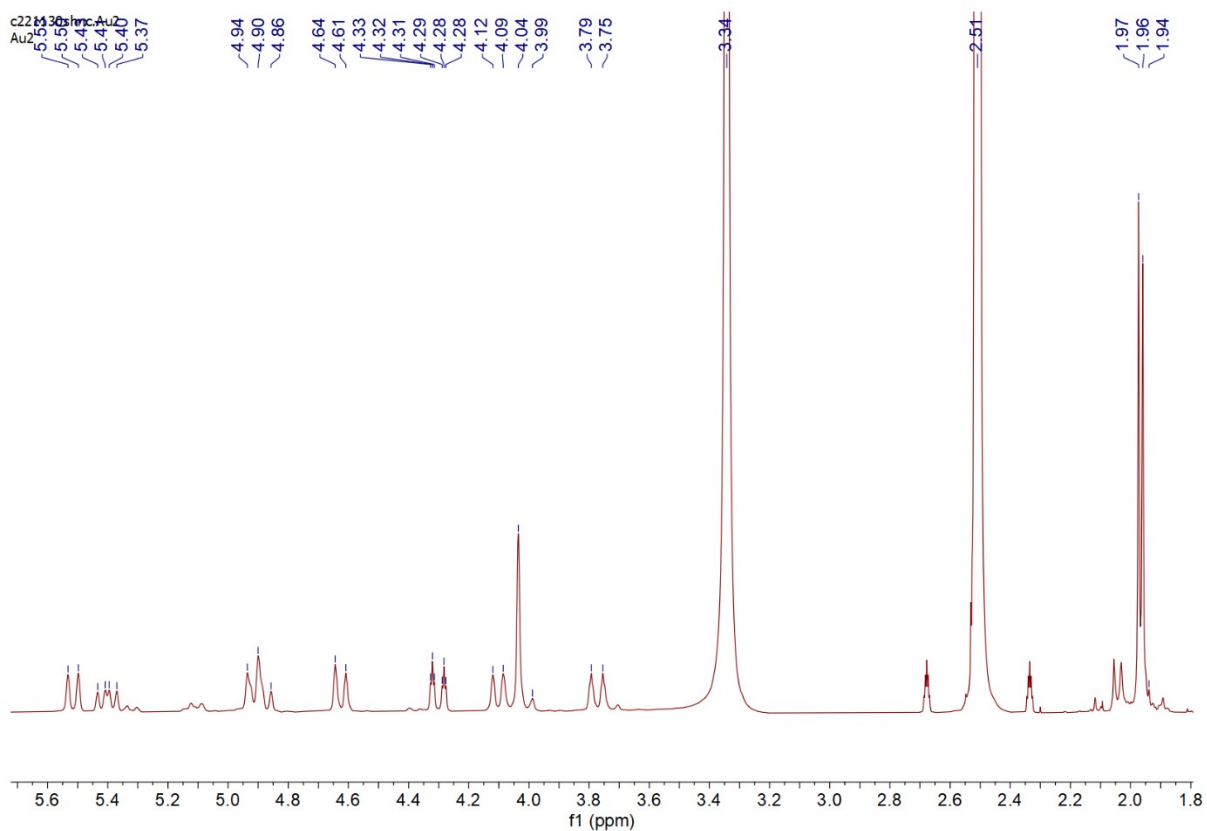


Figure S5. 1H NMR spectrum of compound **2** collected in $(CD_3)_2SO$ (400 MHz).

c221130shnc.Au2
Au2

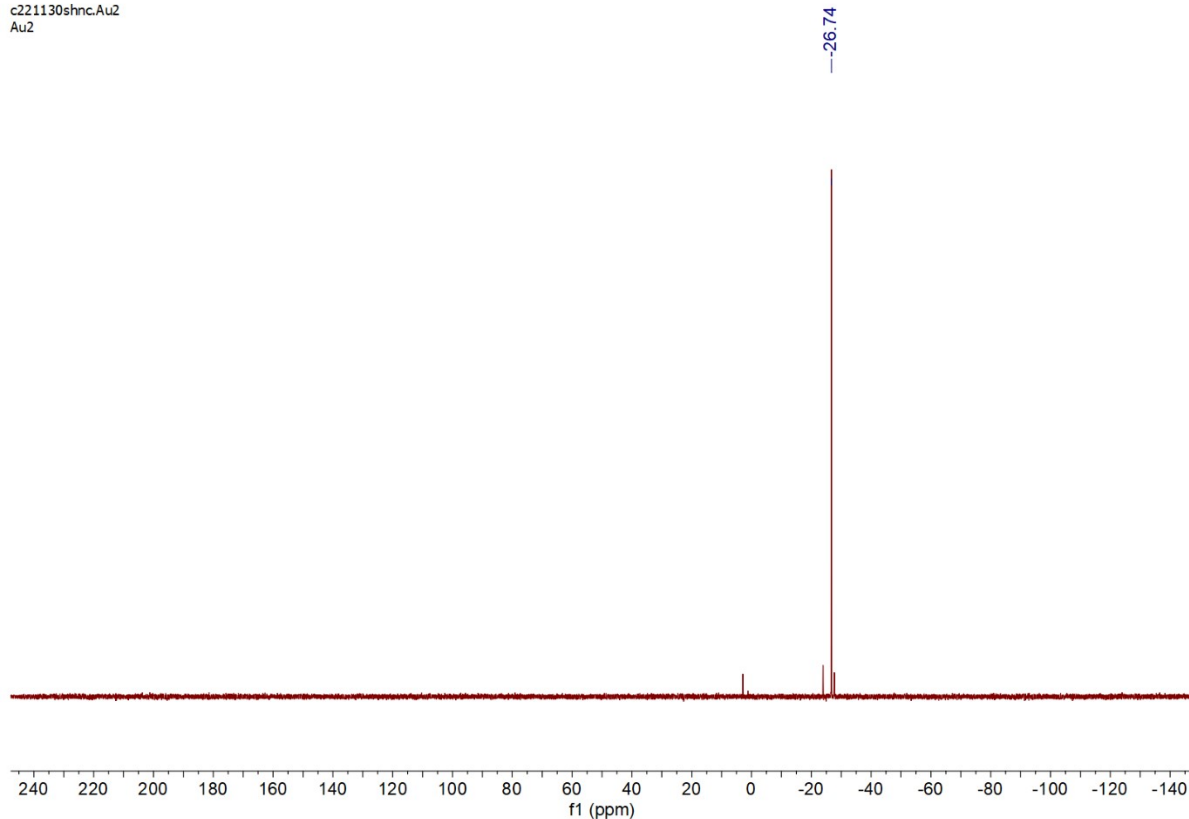


Figure S6. ^{31}P NMR spectrum of compound **2** collected in $(\text{CD}_3)_2\text{SO}$ (400 MHz).

e221216shnc.Au2
NC Au2

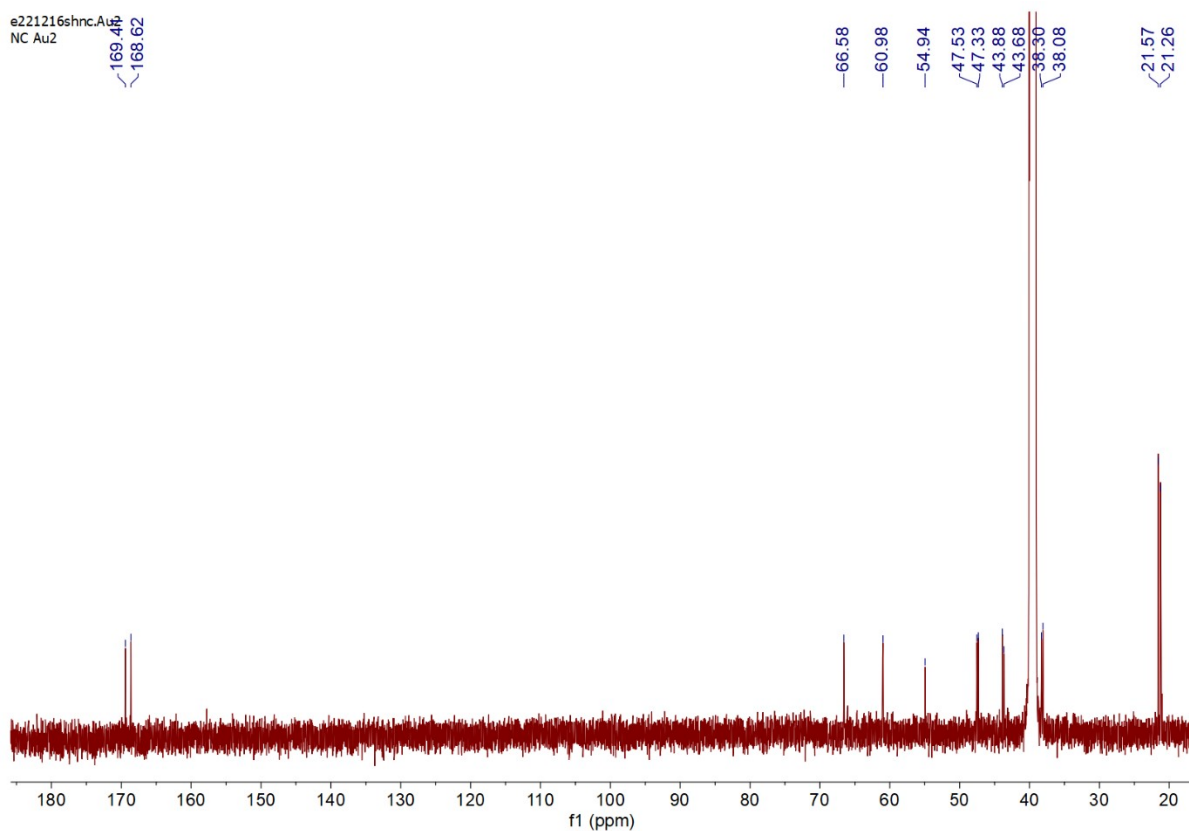


Figure S7. ^{13}C NMR spectrum of compound **2** collected in $(\text{CD}_3)_2\text{SO}$ (600 MHz).

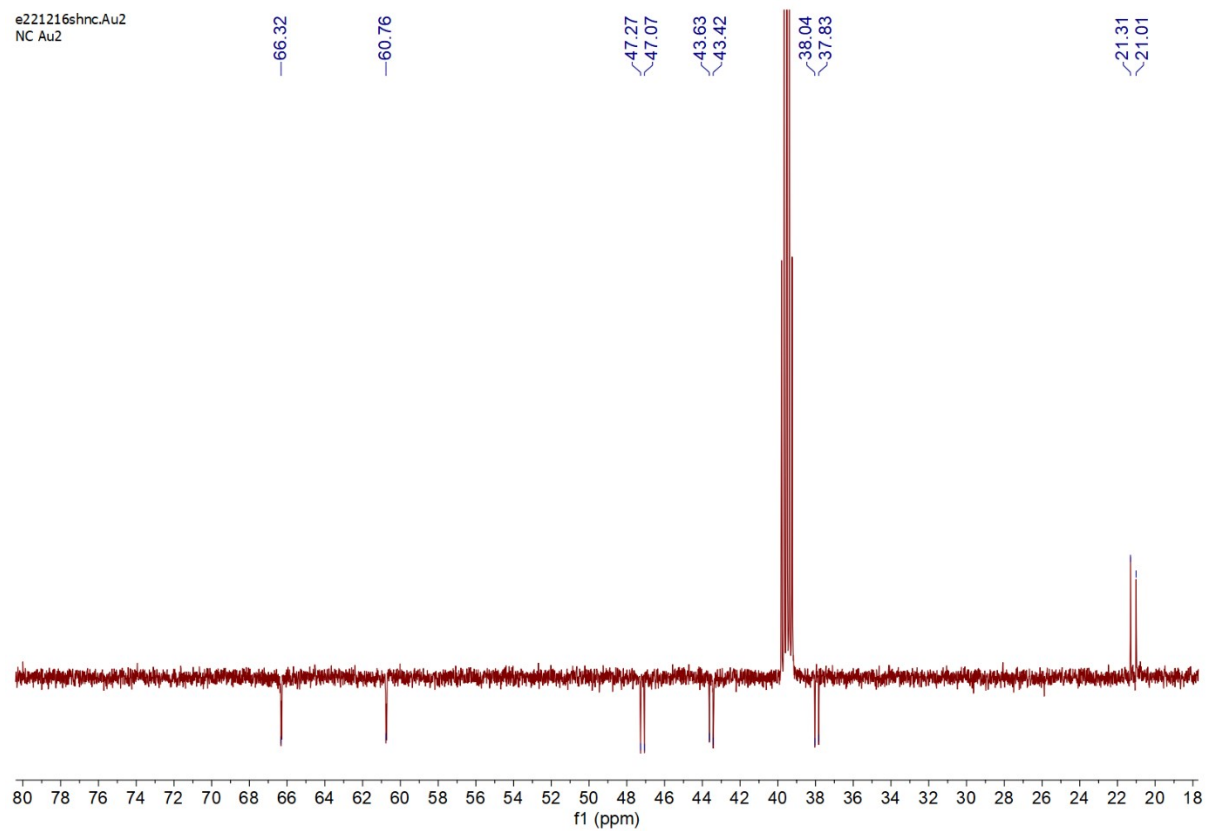


Figure S8. DEPT NMR spectrum of compound **2** collected in $(CD_3)_2SO$ (600 MHz).

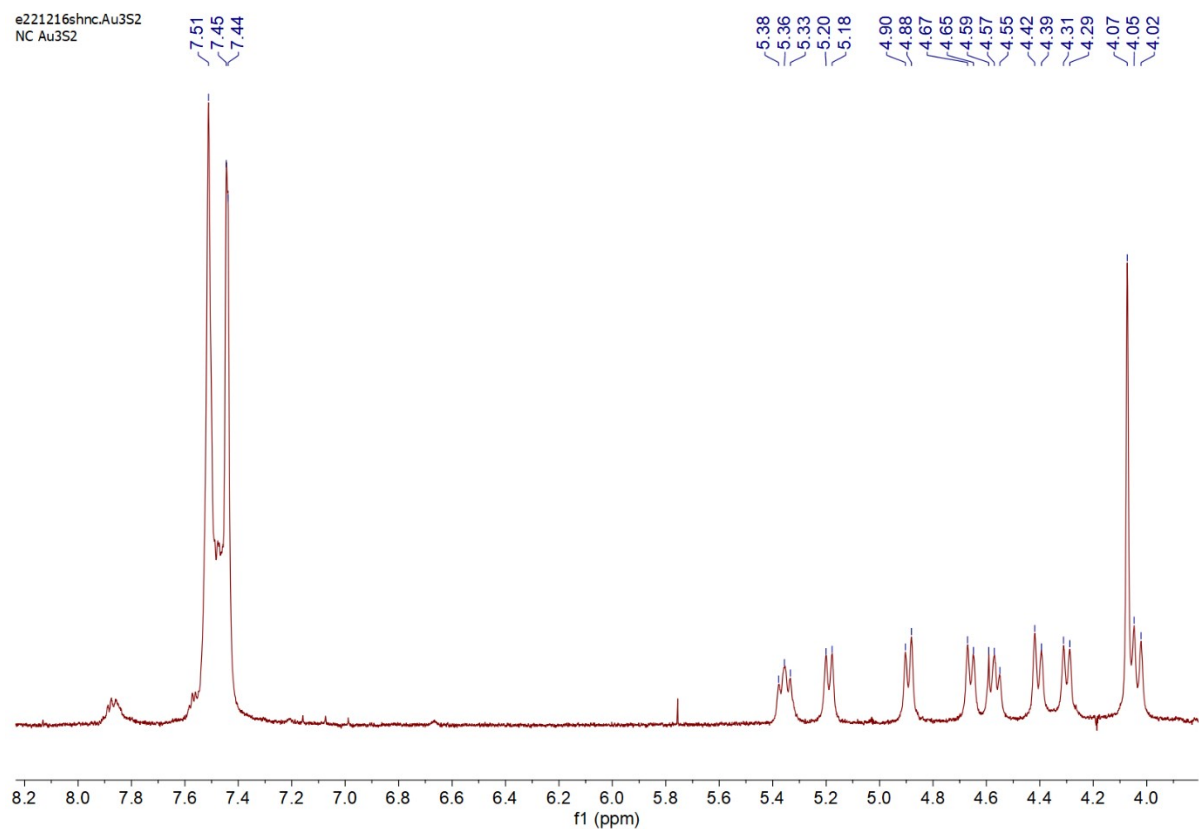


Figure S9. ^1H NMR spectrum of compound **3** collected in $(\text{CD}_3)_2\text{SO}$ (600 MHz).

c221130shnc.Au3S2
Au3S2

-24.53

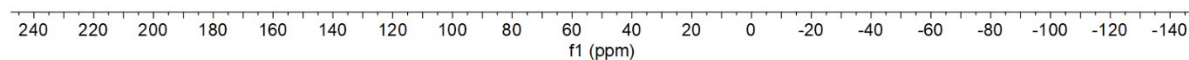


Figure S10. ^{31}P NMR spectrum of compound **3** collected in $(\text{CD}_3)_2\text{SO}$ (400 MHz).

e221212shnc.Au3s3
NC Au3s3

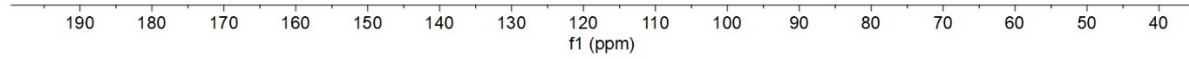


Figure S11. ^{13}C NMR spectrum of compound **3** collected in $(\text{CD}_3)_2\text{SO}$ (600 MHz).

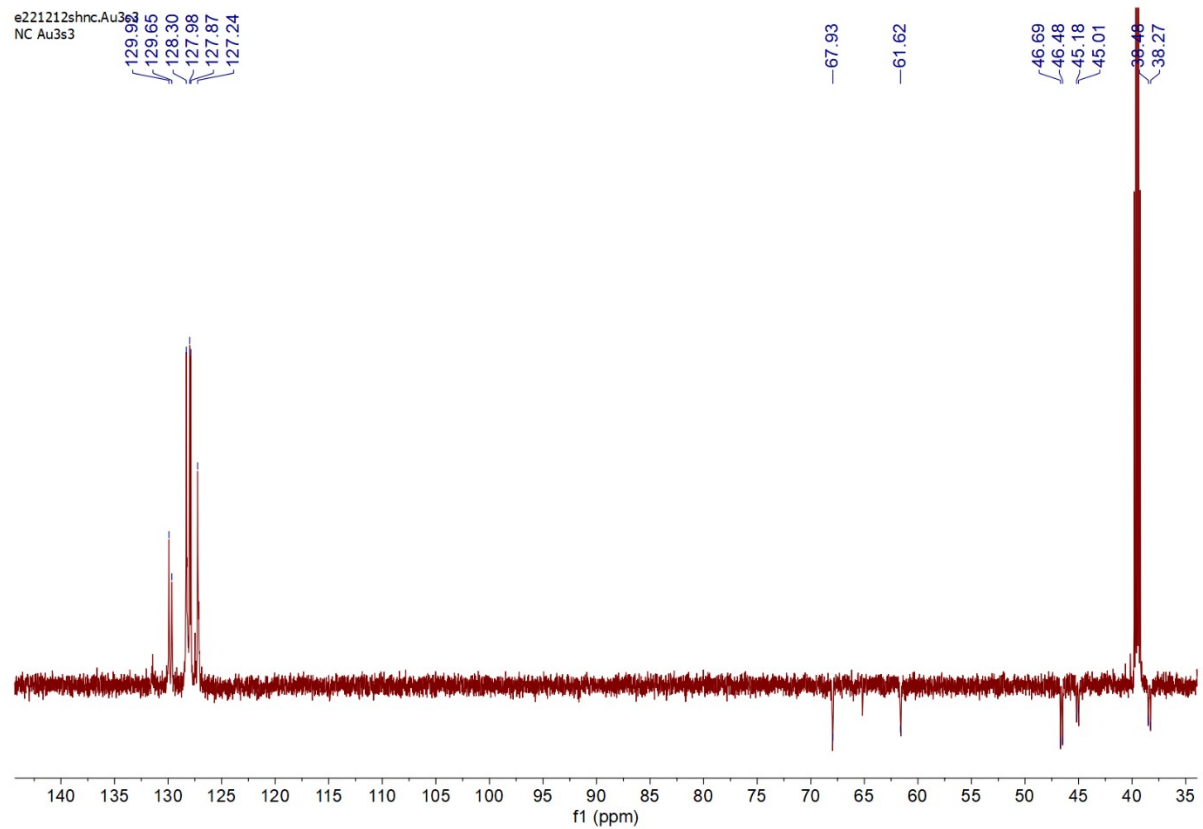


Figure S12. DEPT NMR spectrum of compound **3** collected in $(CD_3)_2SO$ (600 MHz).

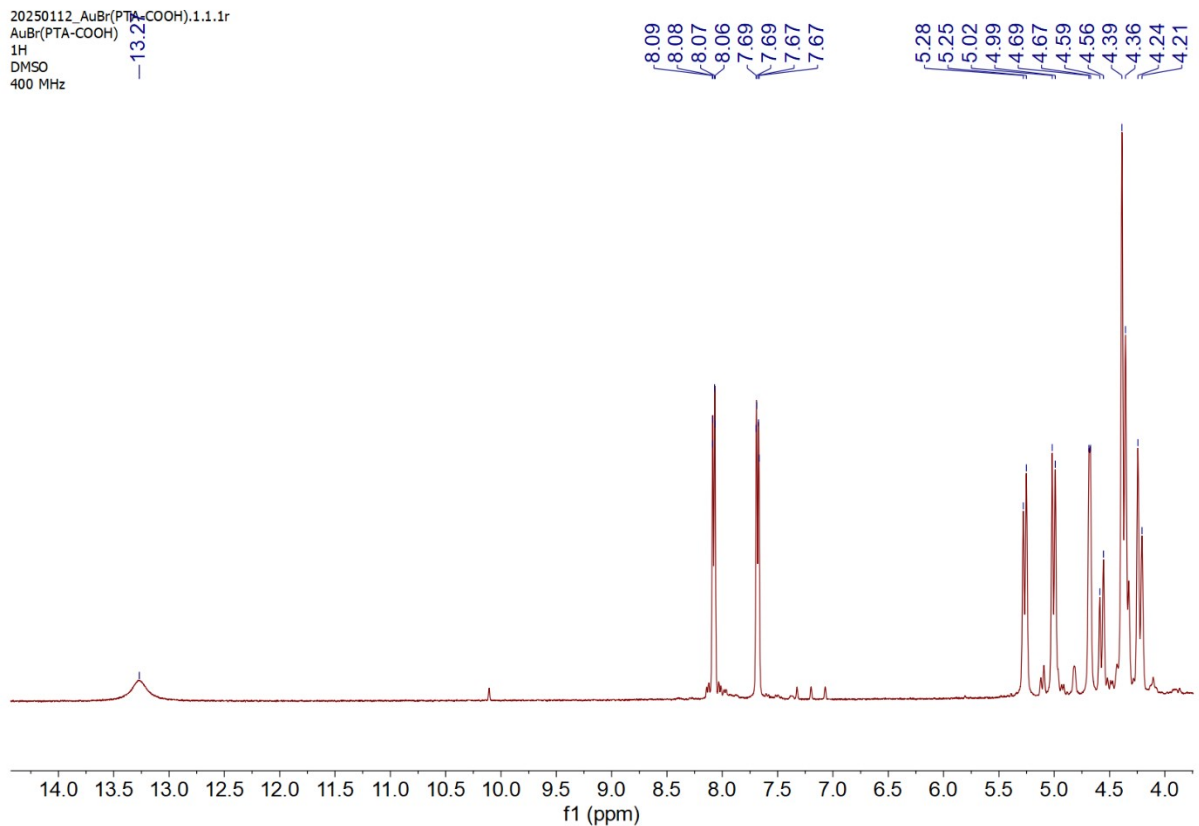


Figure S13. 1H NMR spectrum of compound **4** collected in $(CD_3)_2SO$ (400 MHz).

20250112_AuBr(PTA-COOH).3.1.1r
AuBr(PTA-COOH)
31P
DMSO
400 MHz

—30.83

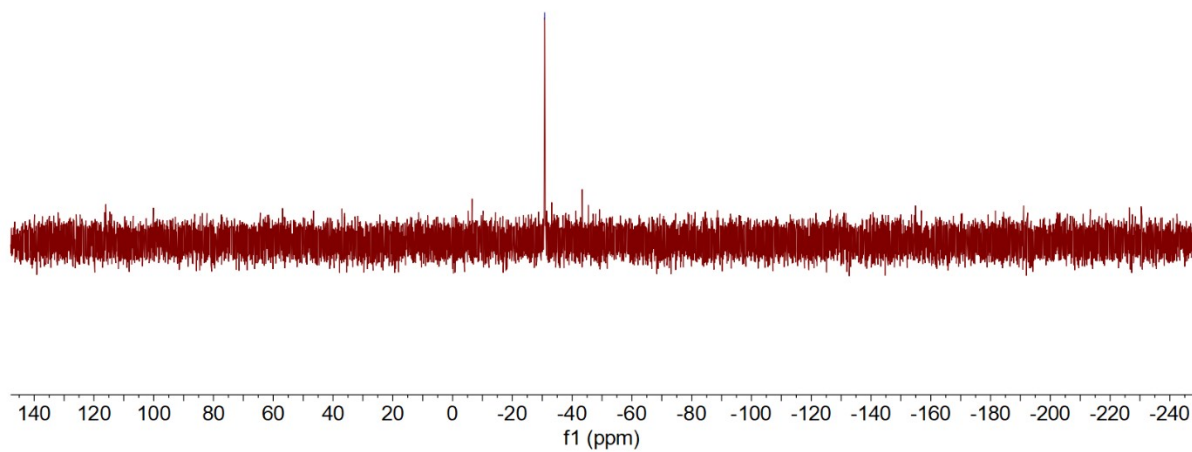


Figure S14. ³¹P NMR spectrum of compound **4** collected in (CD₃)₂SO (400 MHz).

20250112_AuBr(PTA-COOH).4.1.1r
AuBr(PTA-COOH)
13C
DMSO
400 MHz

—166.86

133.40
132.55
129.83
129.78

78.85
78.80
68.75
68.67
63.74
52.12
51.91
47.60
47.37

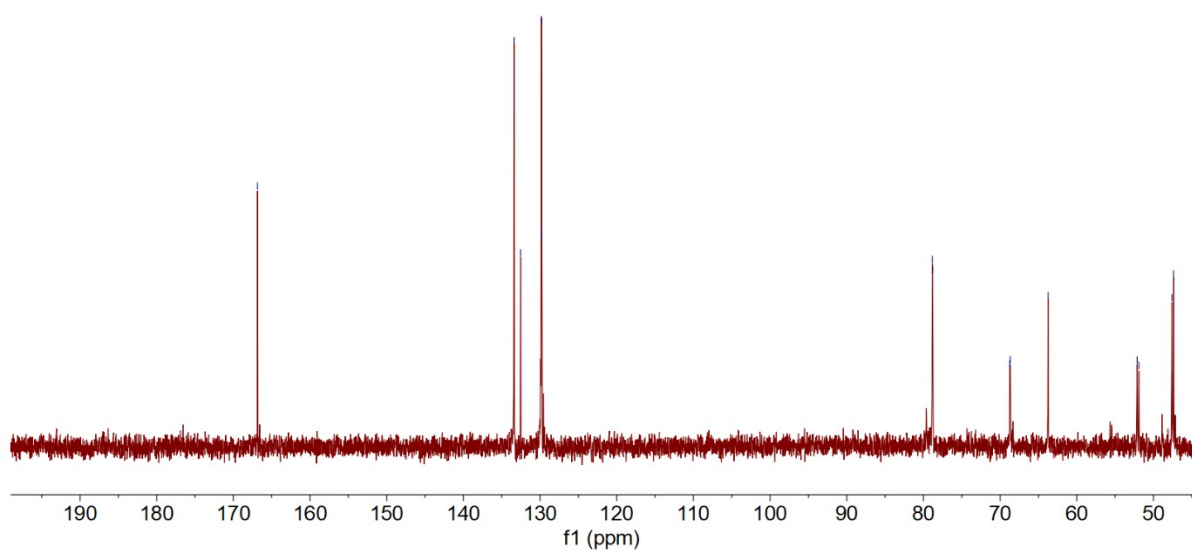


Figure S15. ¹³C NMR spectrum of compound **4** collected in (CD₃)₂SO (400 MHz).

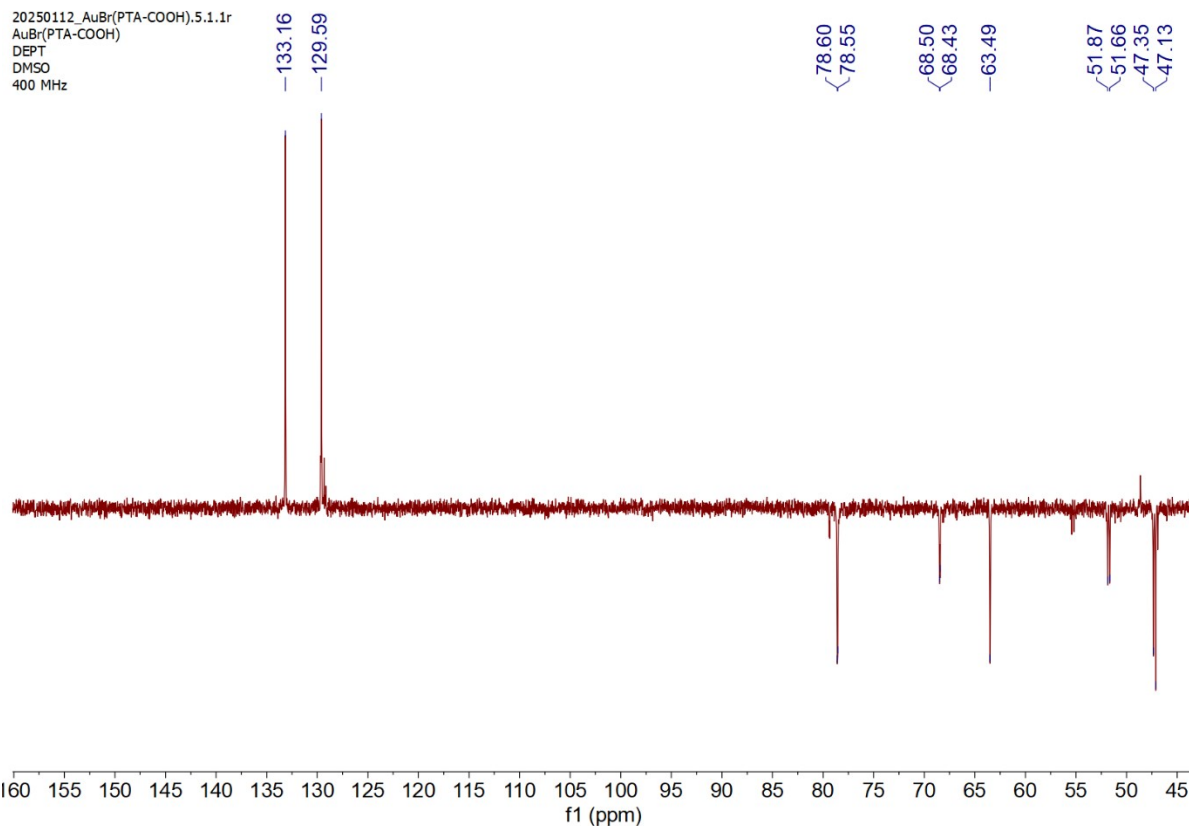


Figure S16. DEPT NMR spectrum of compound **4** collected in $(CD_3)_2SO$ (400 MHz).

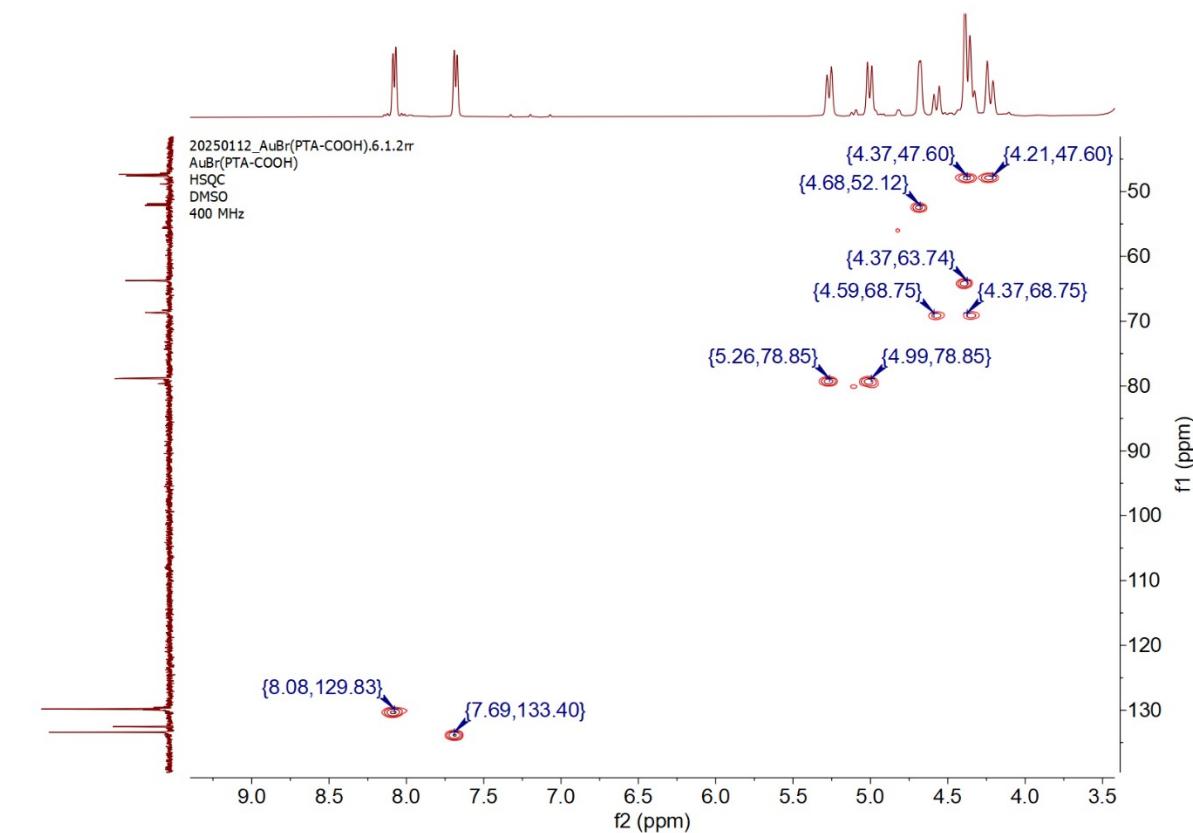


Figure S17. HSQC NMR spectrum of compound **4** collected in $(CD_3)_2SO$ (400 MHz).

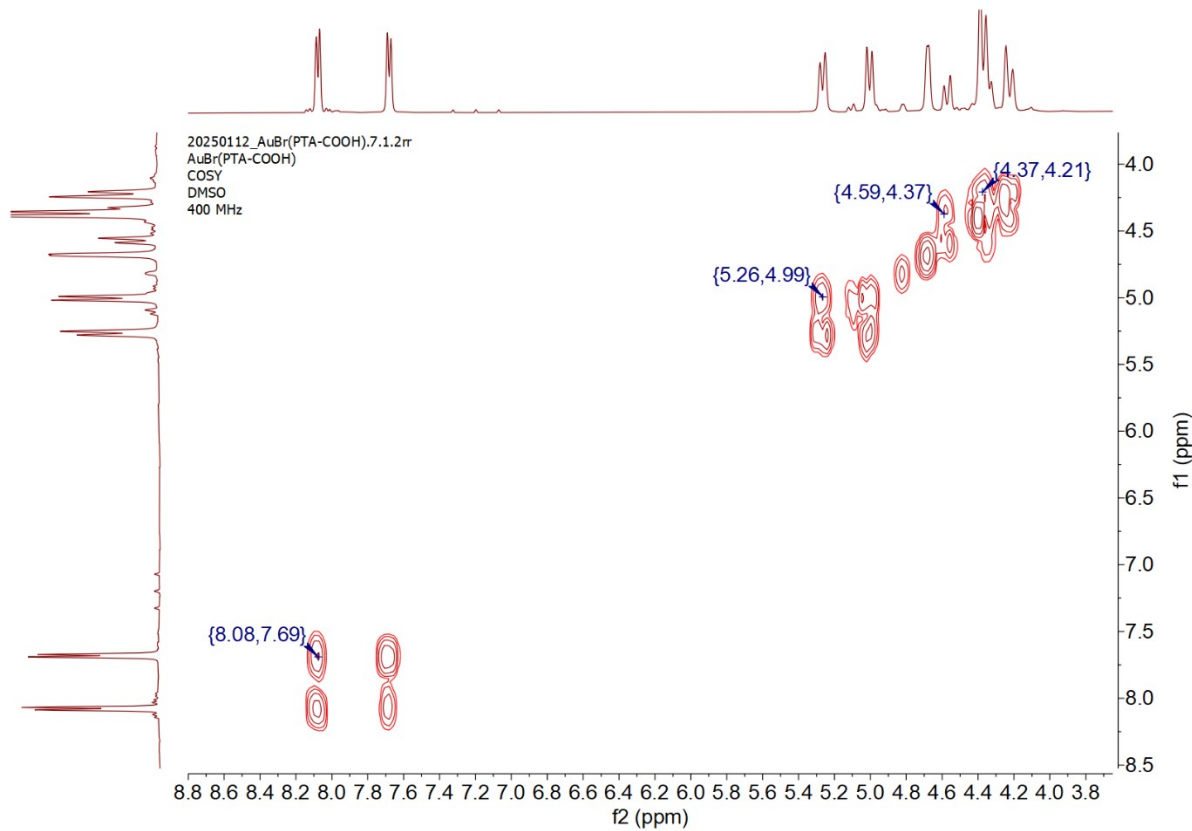


Figure S18. COSY NMR spectrum of compound **4** collected in $(CD_3)_2SO$ (400 MHz).

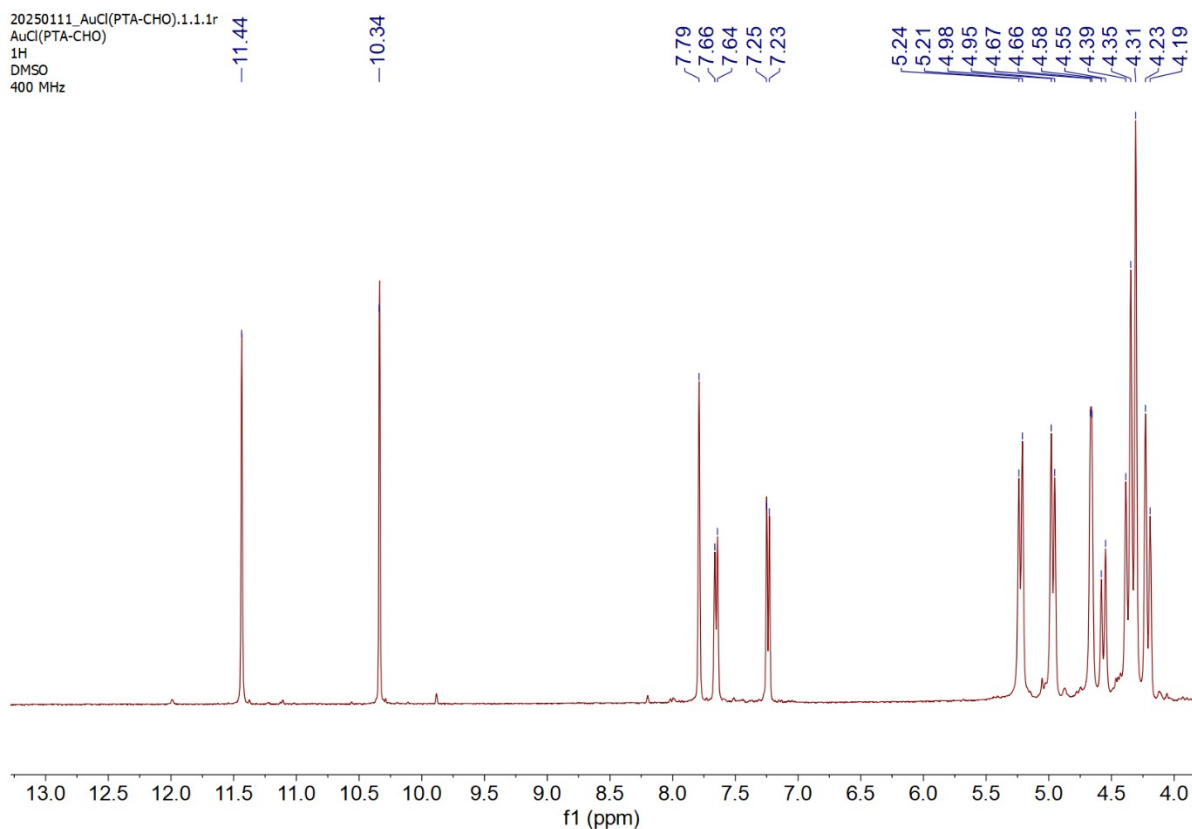


Figure S19. 1H NMR spectrum of compound **5** collected in $(CD_3)_2SO$ (400 MHz).

20250111_AuCl(PTA-CHO).2.1.1r
AuCl(PTA-CHO)
31P
DMSO
400 MHz

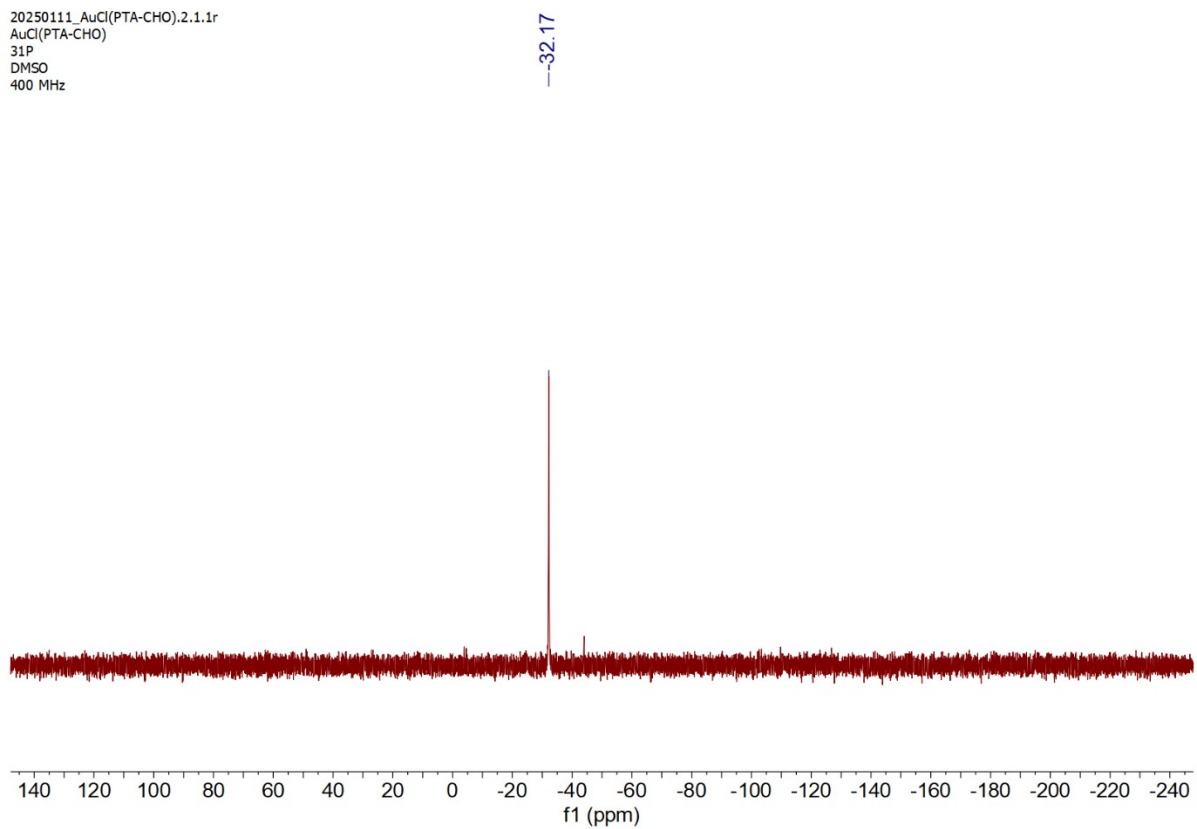


Figure S20. ³¹P NMR spectrum of compound **5** collected in (CD₃)₂SO (400 MHz).

20250111_AuCl(PTA-CHO).3.1.1r
AuCl(PTA-CHO)
13C
DMSO
400 MHz

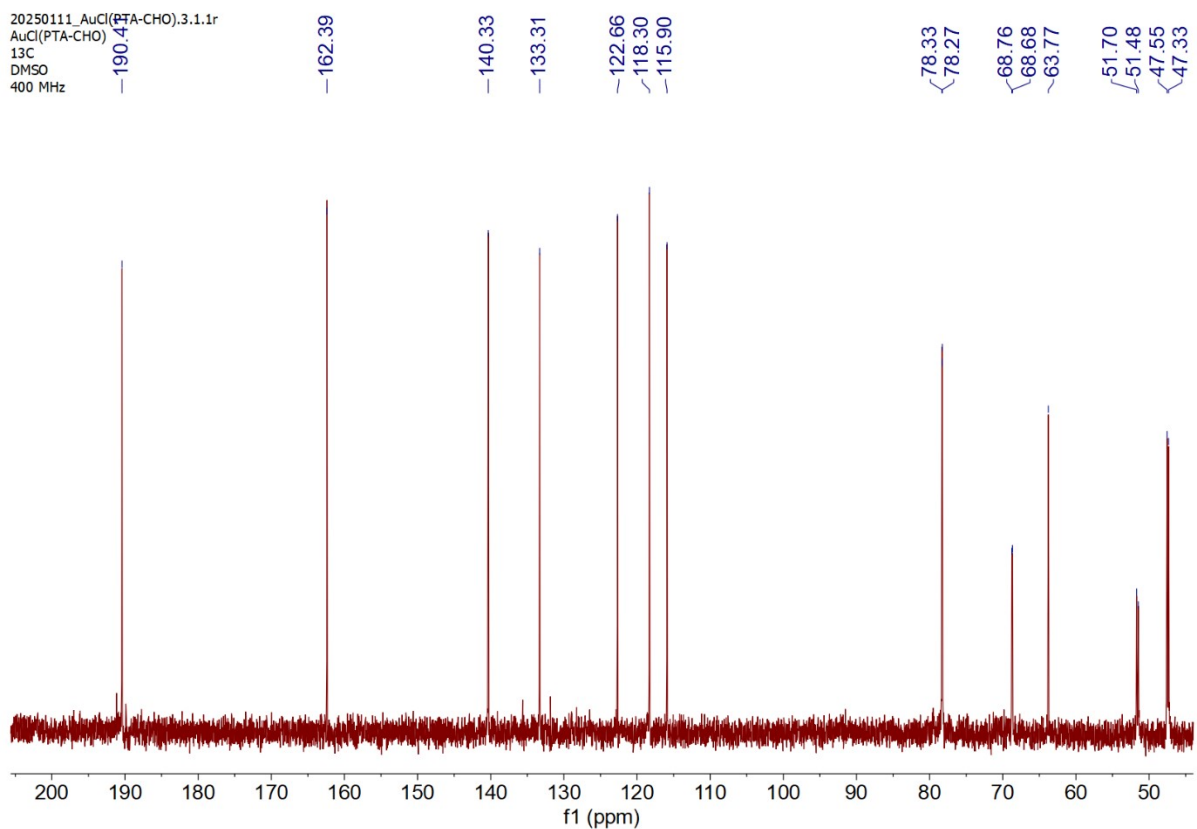


Figure S21. ¹³C NMR spectrum of compound **5** collected in (CD₃)₂SO (400 MHz).

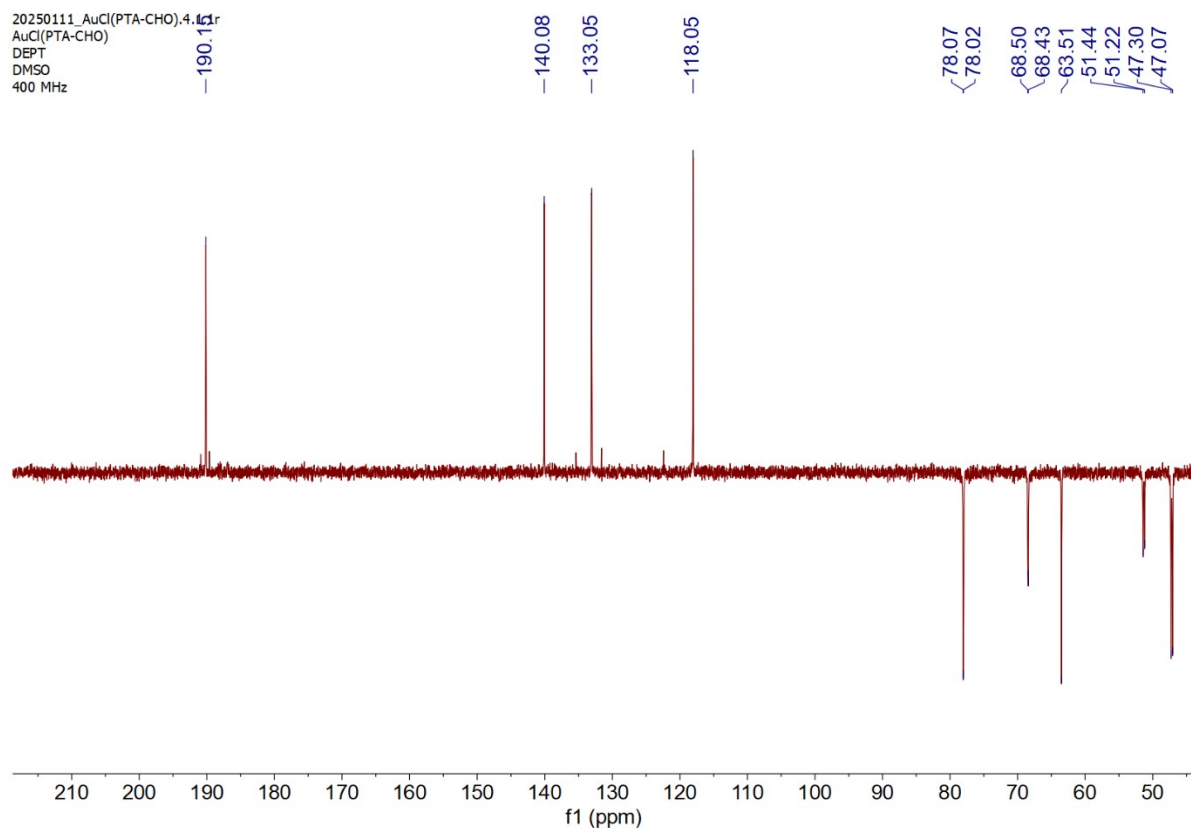


Figure S22. DEPT NMR spectrum of compound **5** collected in $(CD_3)_2SO$ (400 MHz).

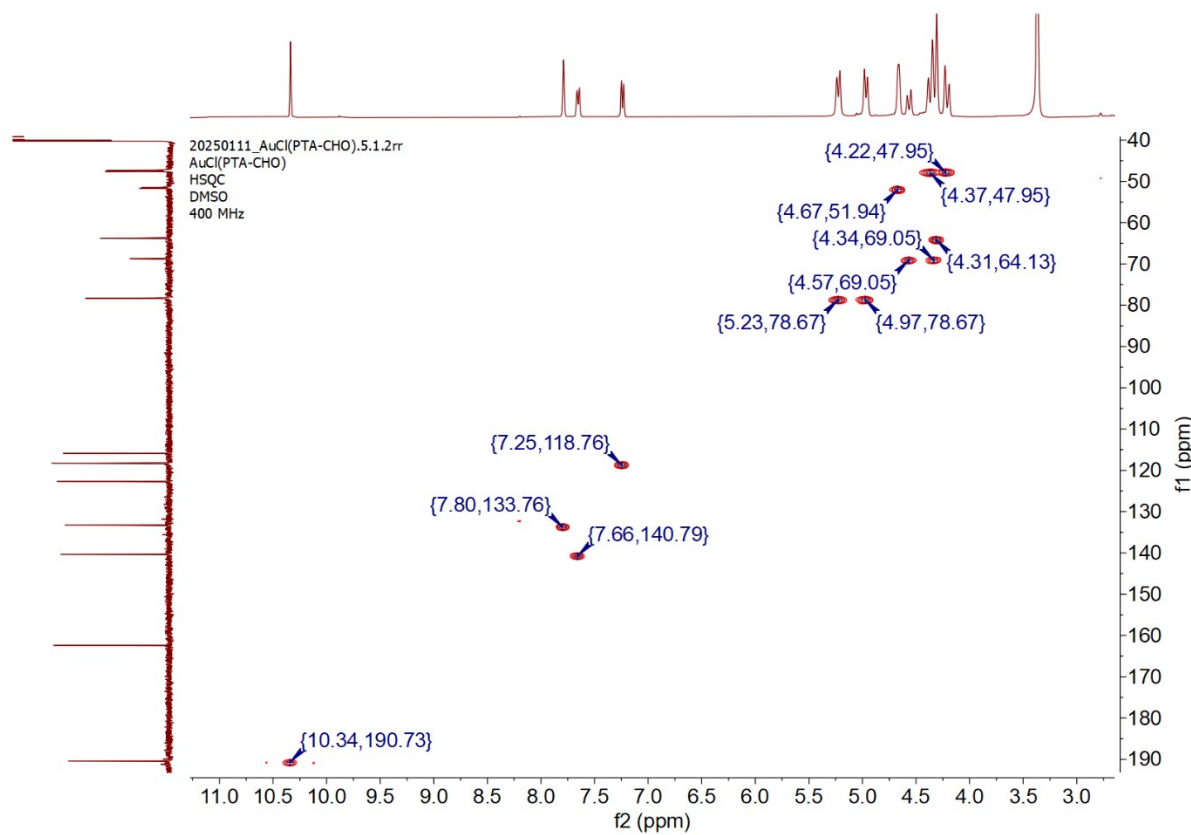


Figure S23. HSQC NMR spectrum of compound **5** collected in $(CD_3)_2SO$ (400 MHz).

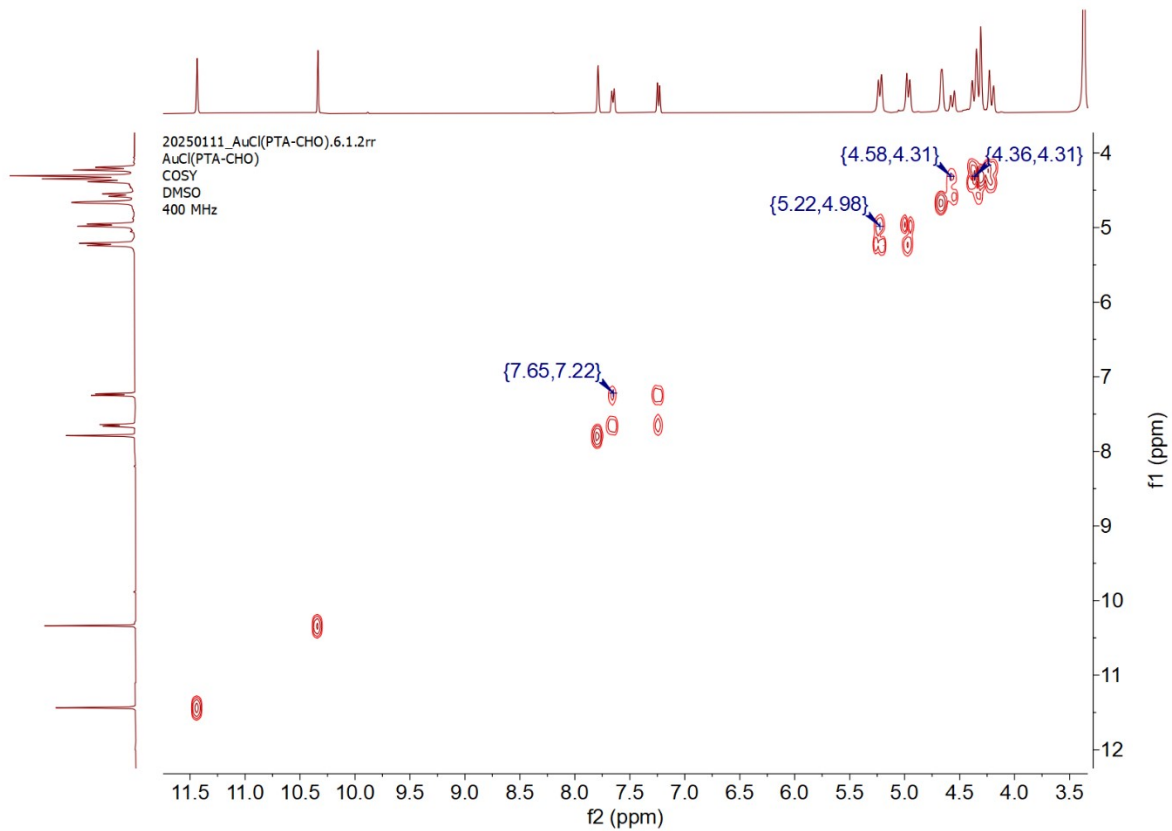


Figure S24. COSY NMR spectrum of compound **5** collected in $(CD_3)_2SO$ (400 MHz).

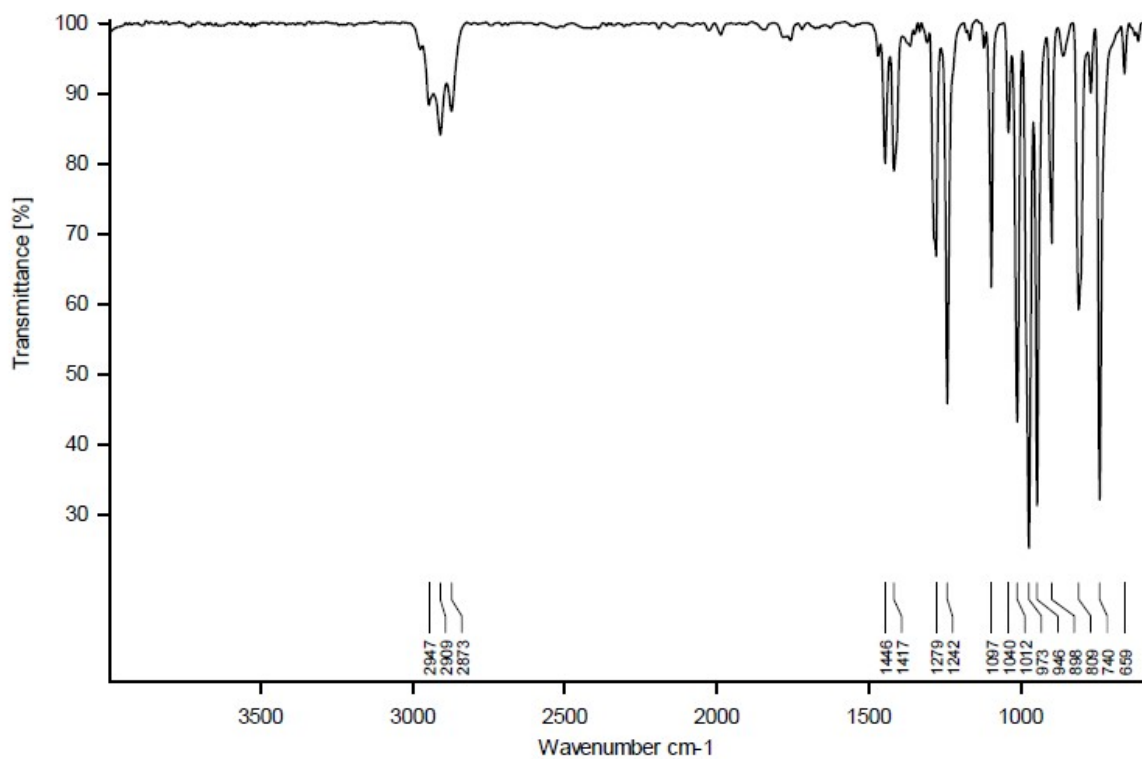


Figure S25. ATR-FTIR spectrum of compound **1**.

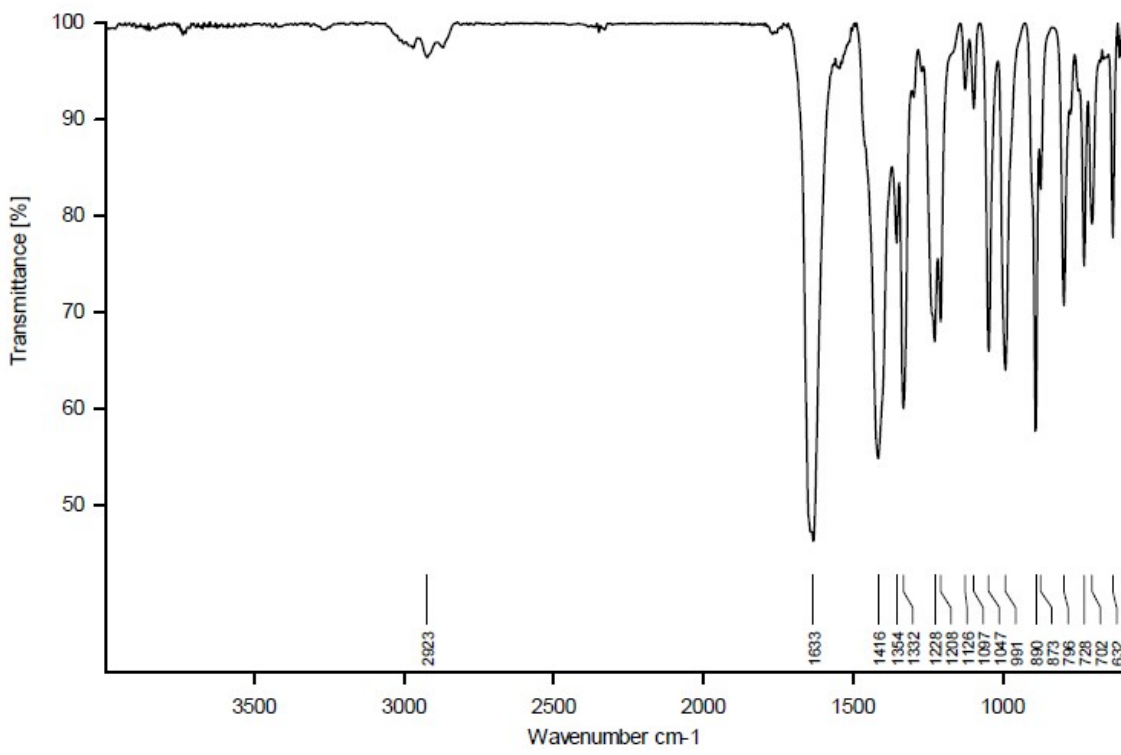


Figure S26. ATR-FTIR spectrum of compound 2.

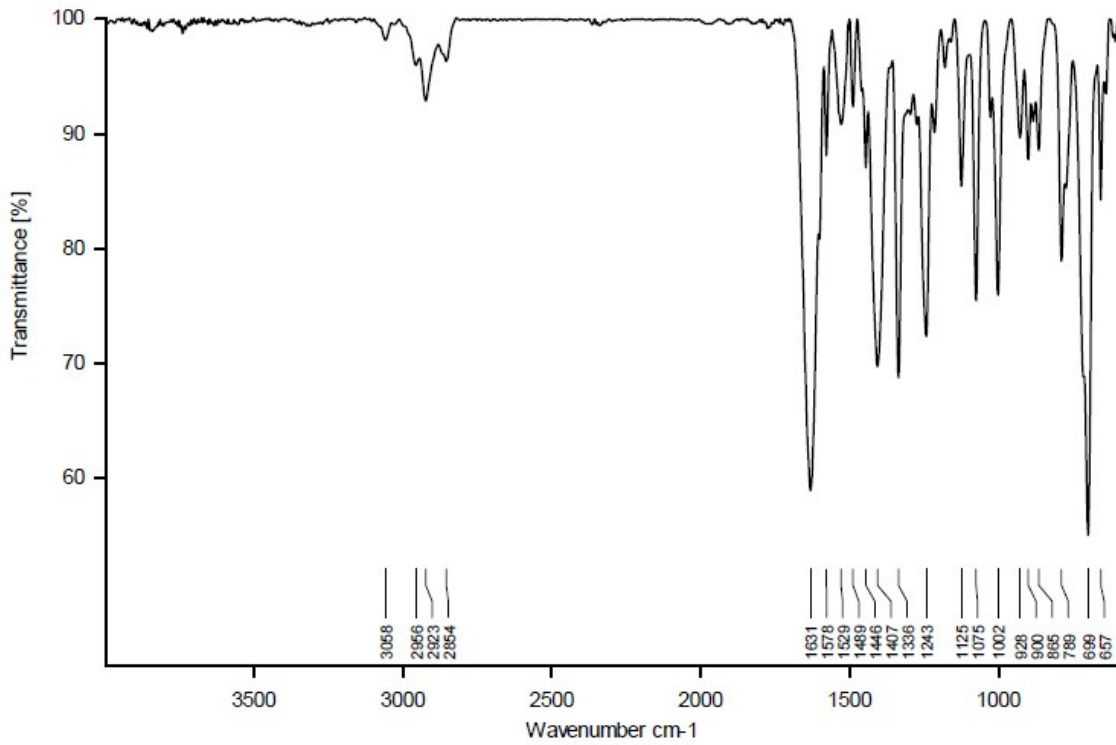


Figure S27. ATR-FTIR spectrum of compound 3.

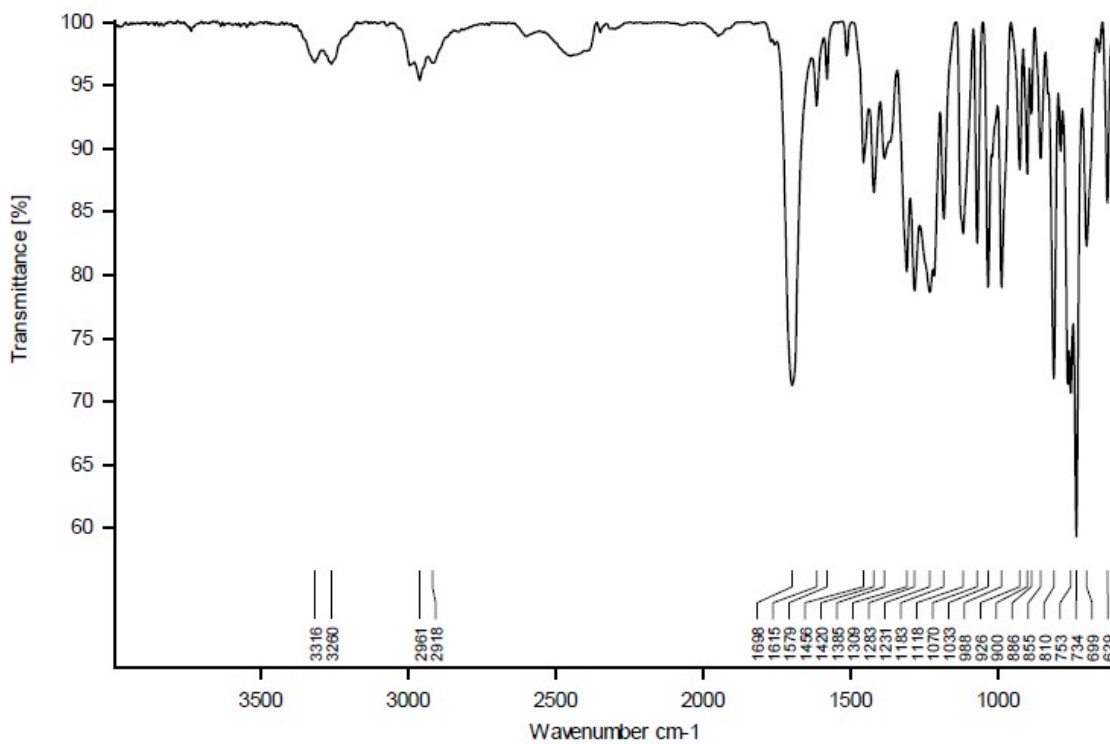


Figure S28. ATR-FTIR spectrum of compound 4.

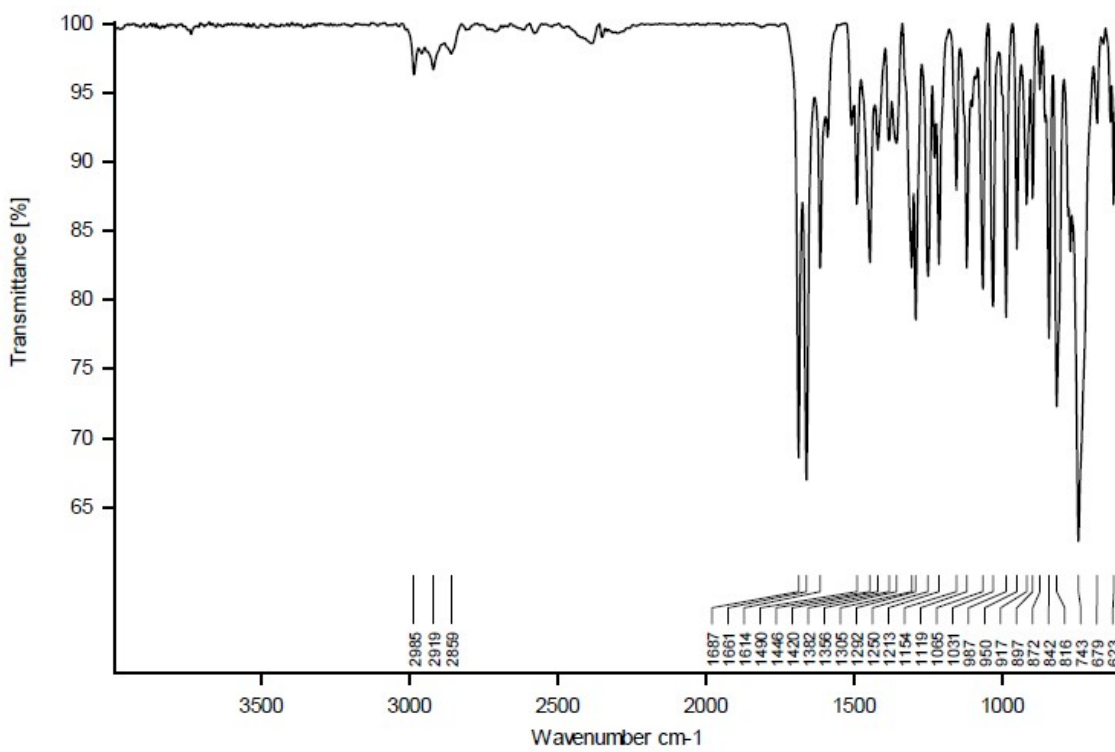


Figure S29. ATR-FTIR spectrum of compound 5.

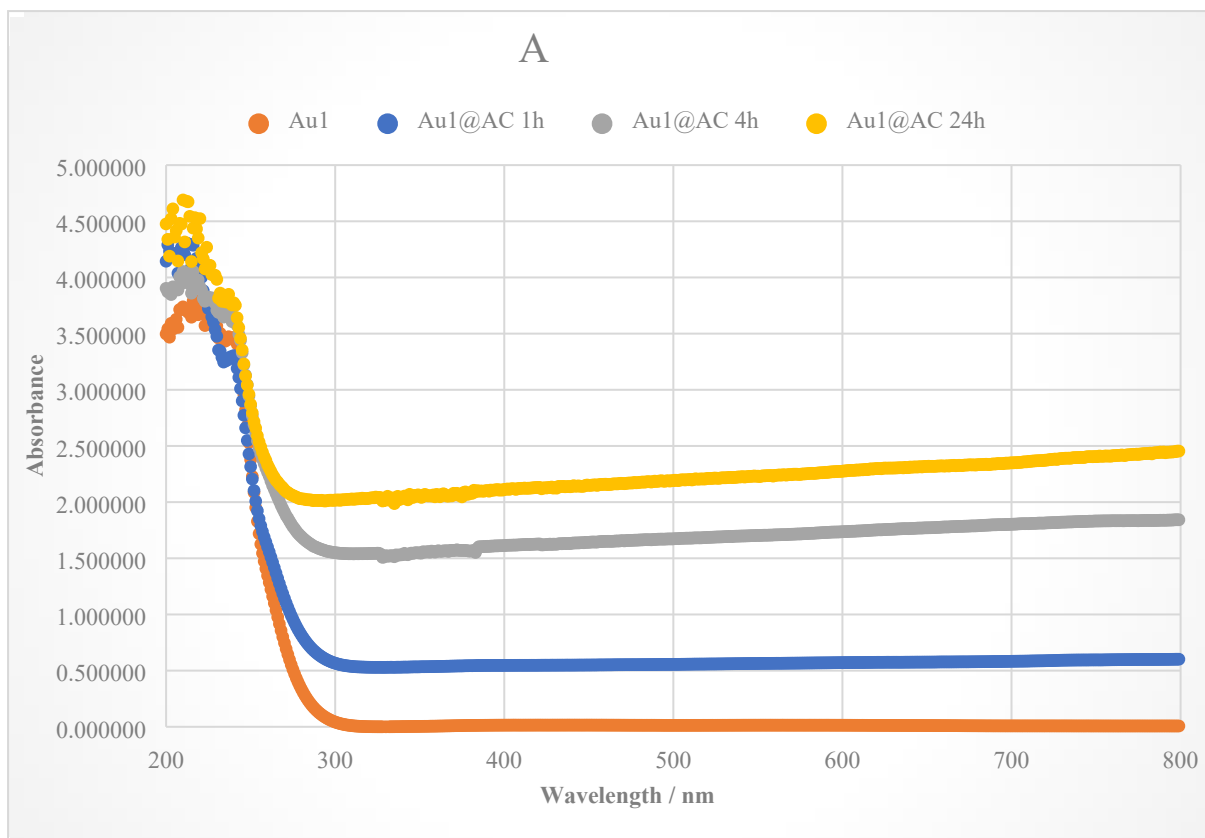


Figure S30. Heterogenization UV-Vis profiles throughout time of the supernatant from compound **1** on AC.

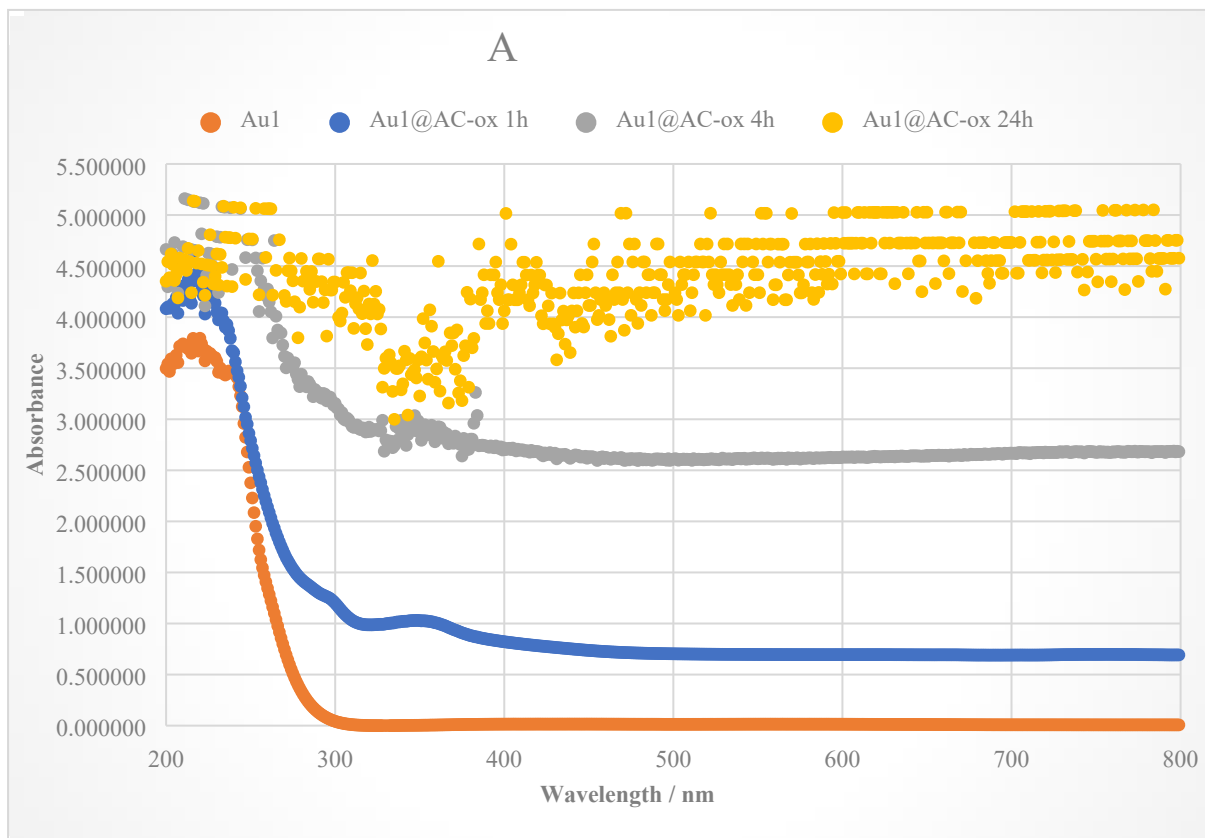


Figure S31. Heterogenization UV-Vis profiles throughout time of the supernatant from compound **1** on AC-ox.

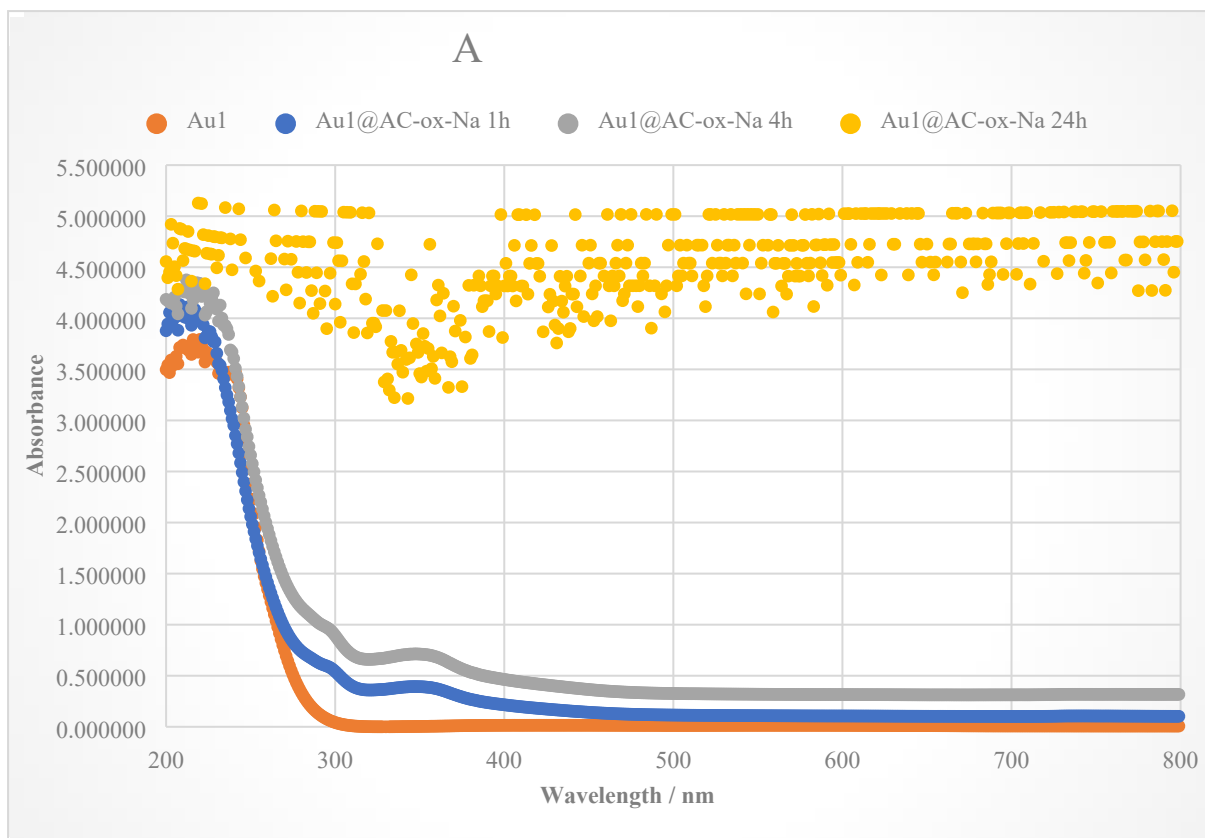


Figure S32. Heterogenization UV-Vis profiles throughout time of the supernatant from compound **1** on AC-ox-Na.

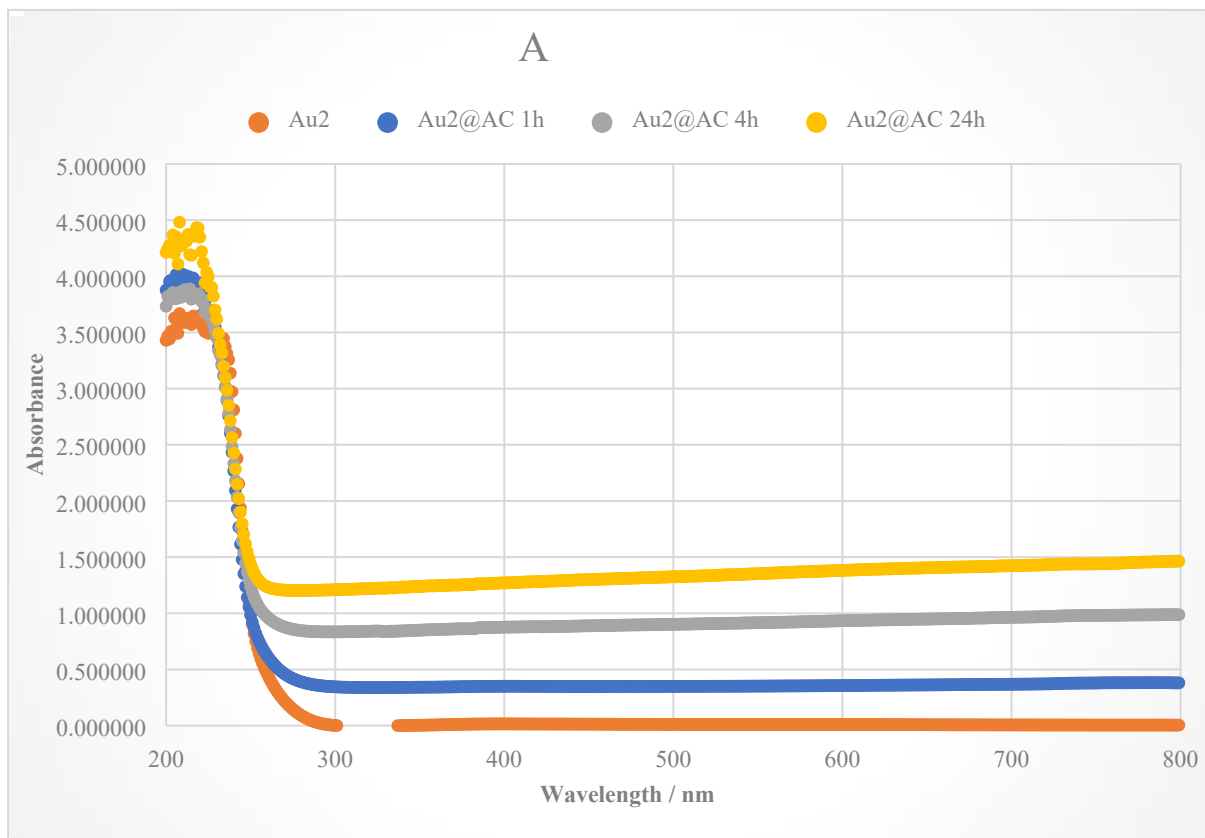


Figure S33. Heterogenization UV-Vis profiles throughout time of the supernatant from compound **2** on AC.

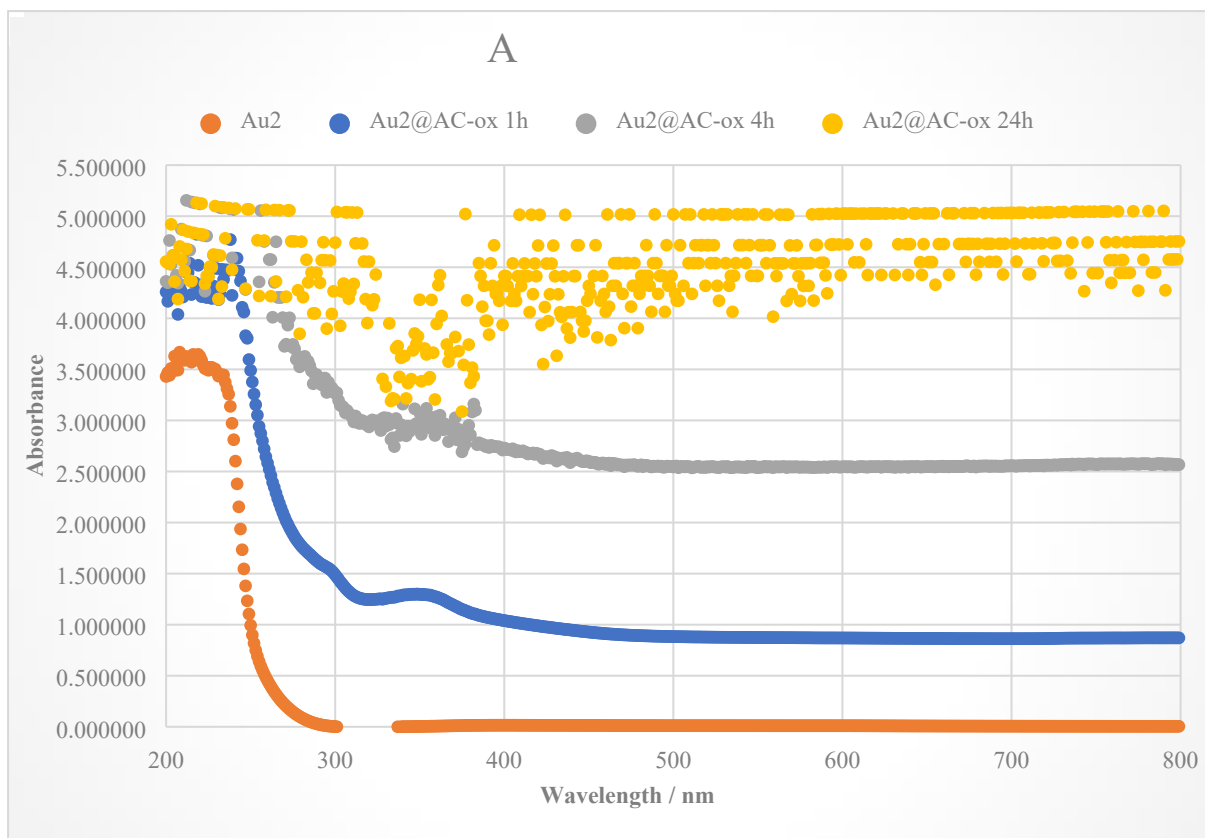


Figure S34. Heterogenization UV-Vis profiles throughout time of the supernatant from compound 2 on AC-ox.

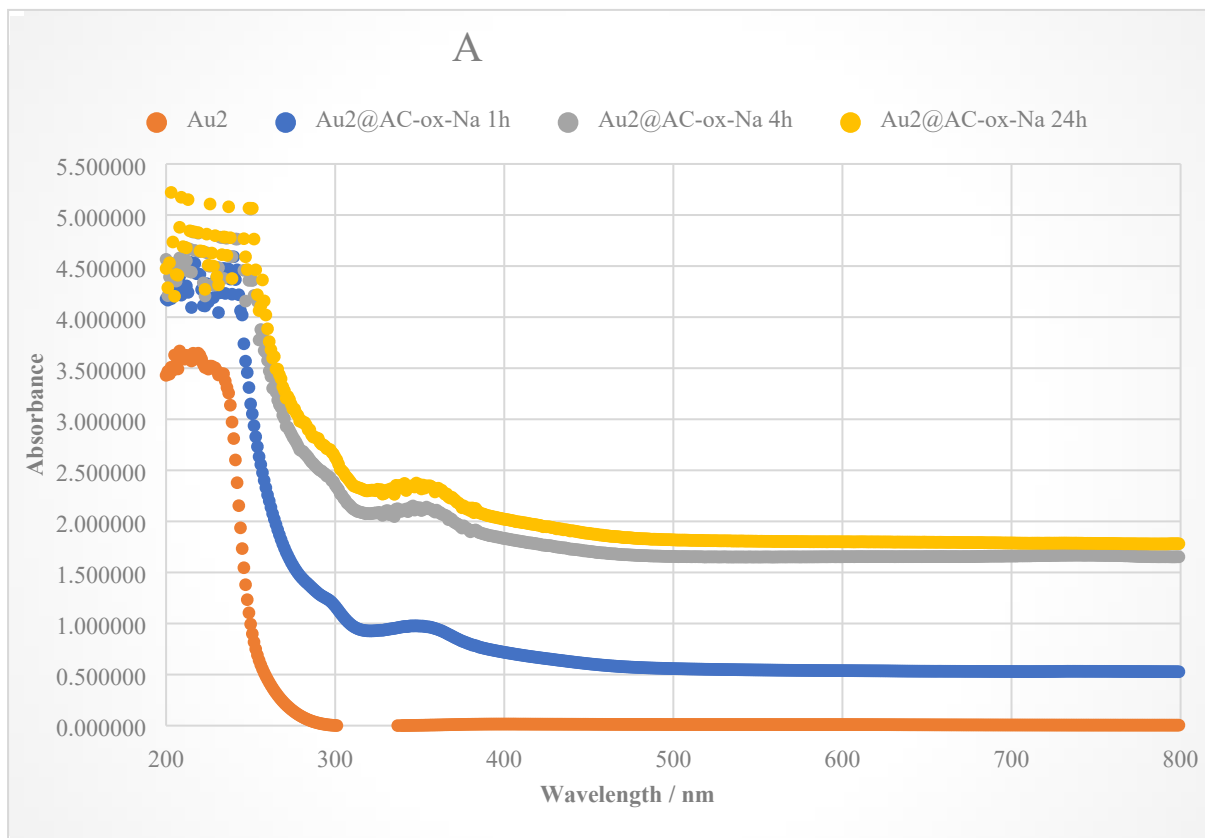


Figure S35. Heterogenization UV-Vis profiles throughout time of the supernatant from compound 2 on AC-ox-Na.

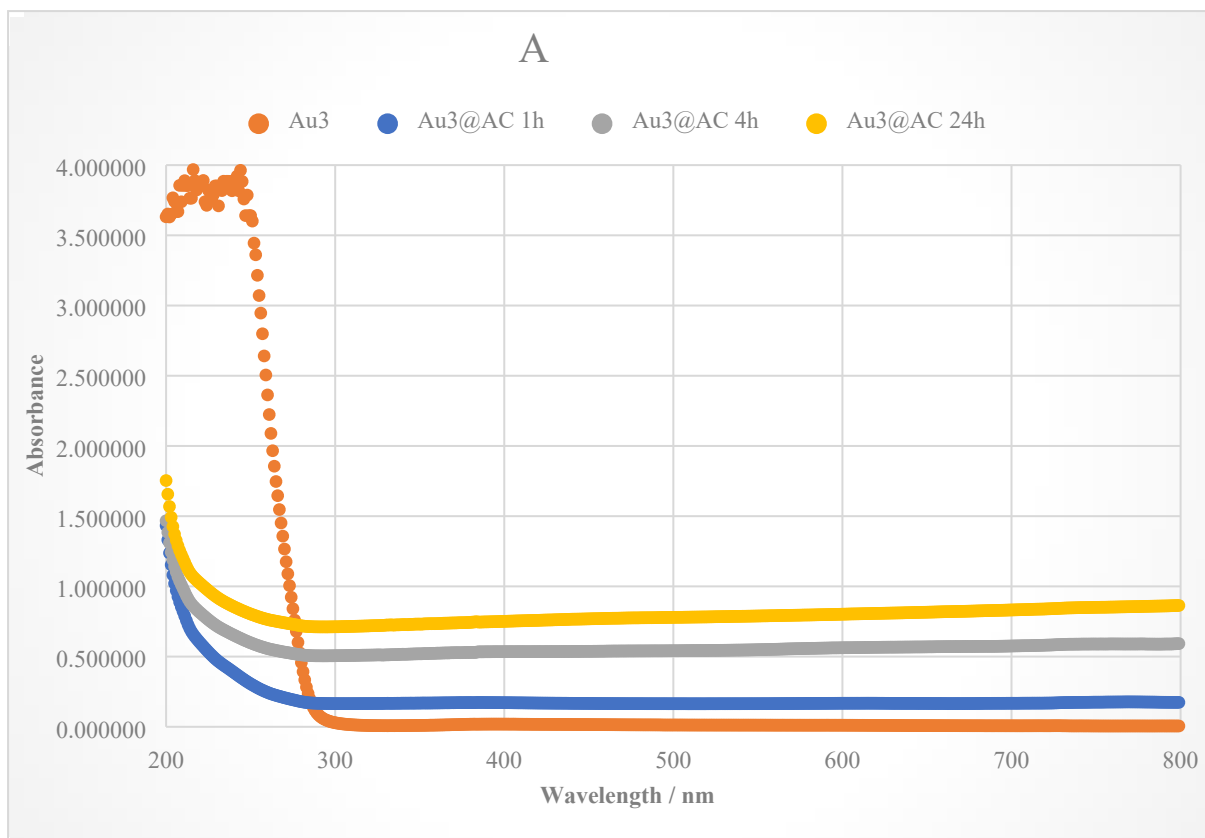


Figure S36. Heterogenization UV-Vis profiles throughout time of the supernatant from compound **3** on AC.

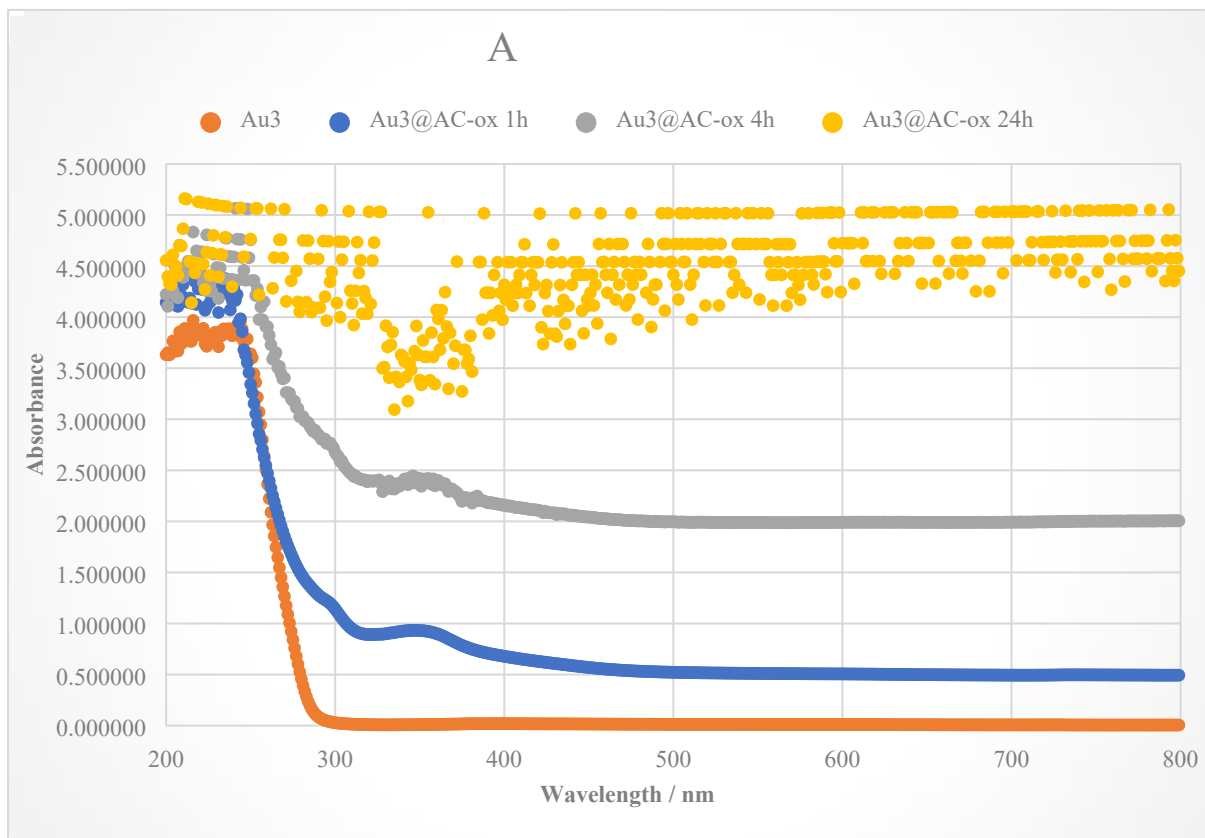


Figure S37. Heterogenization UV-Vis profiles throughout time of the supernatant from compound **3** on AC-ox.

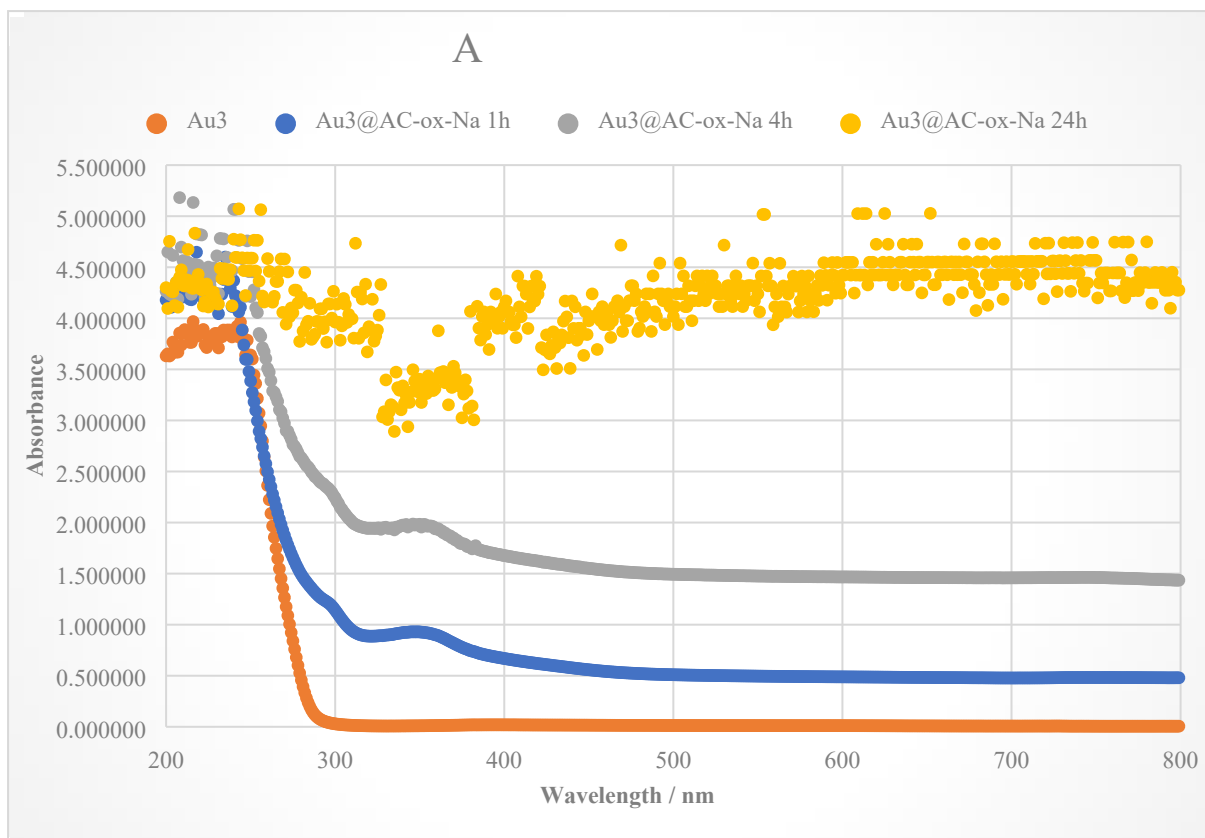


Figure S38. Heterogenization UV-Vis profiles throughout time of the supernatant from compound **3** on AC-ox-Na.

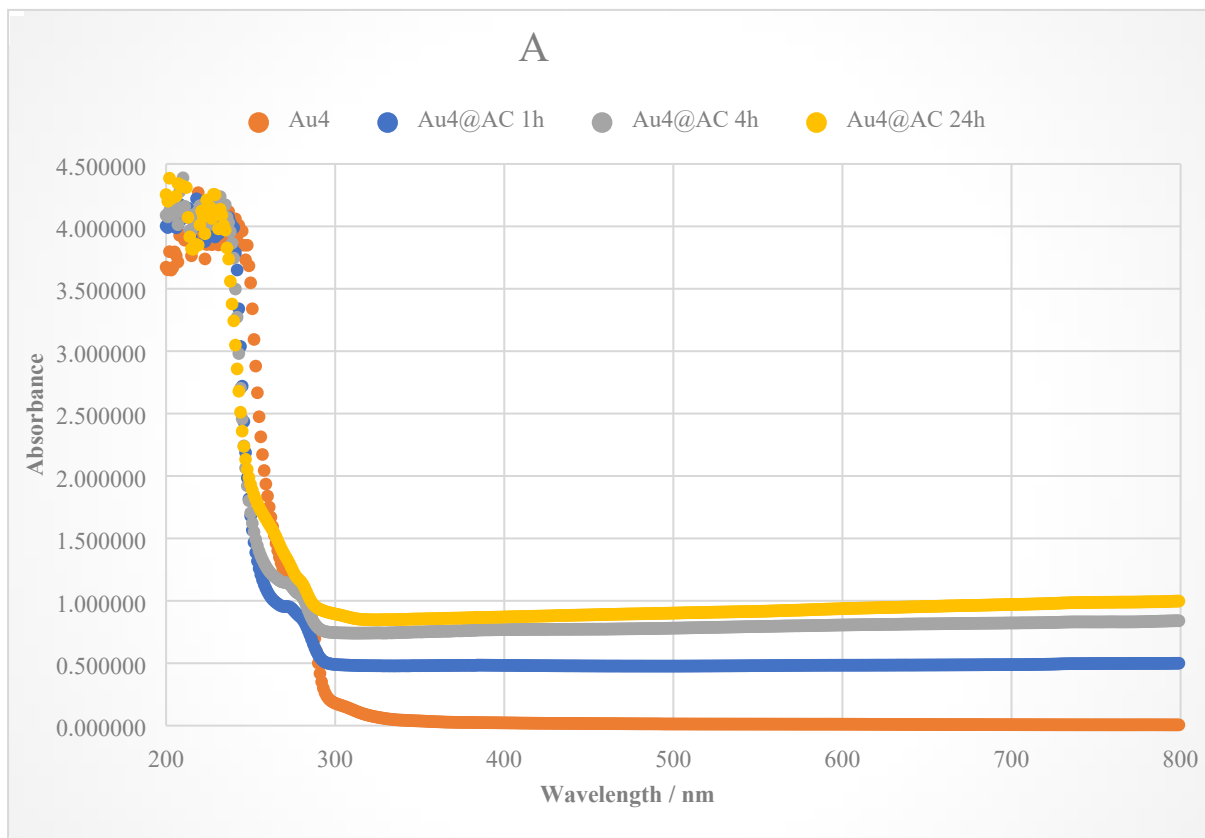


Figure S39. Heterogenization UV-Vis profiles throughout time of the supernatant from compound **4** on AC.

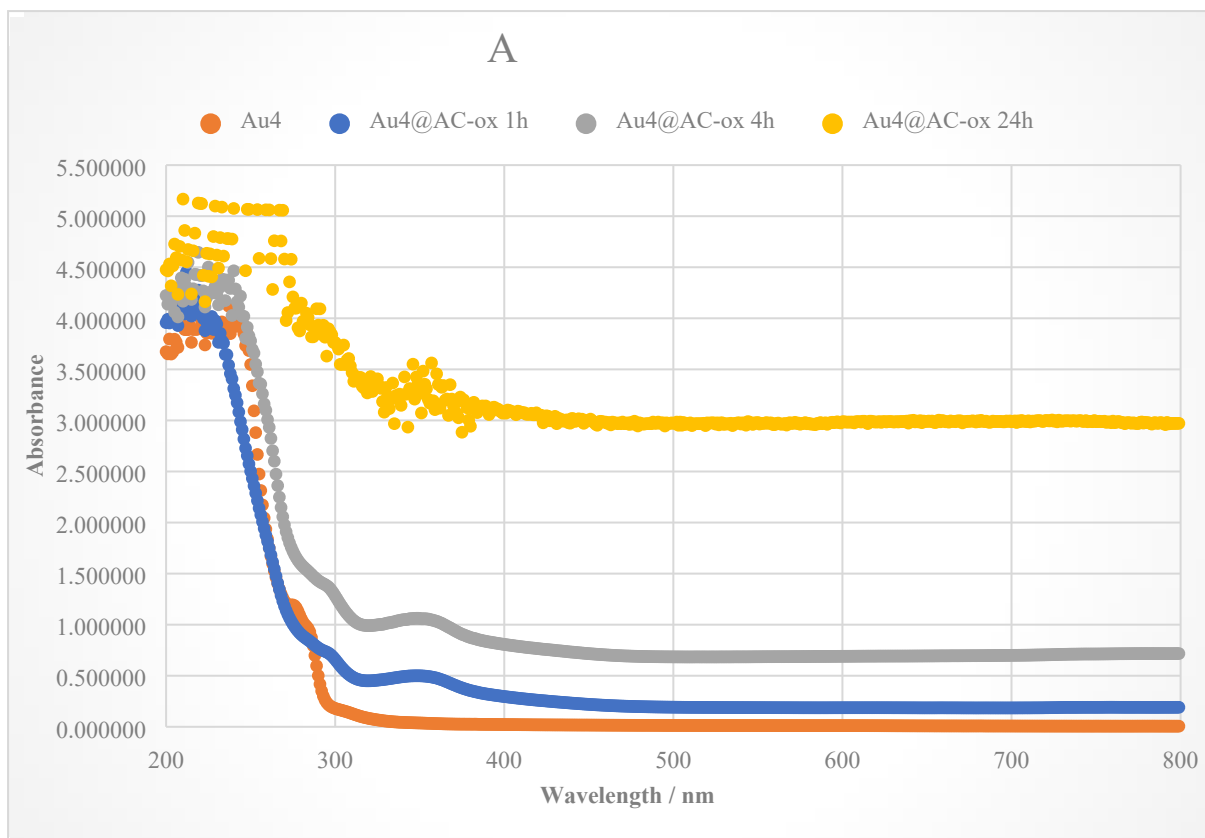


Figure S40. Heterogenization UV-Vis profiles throughout time of the supernatant from compound **4** on AC-ox.

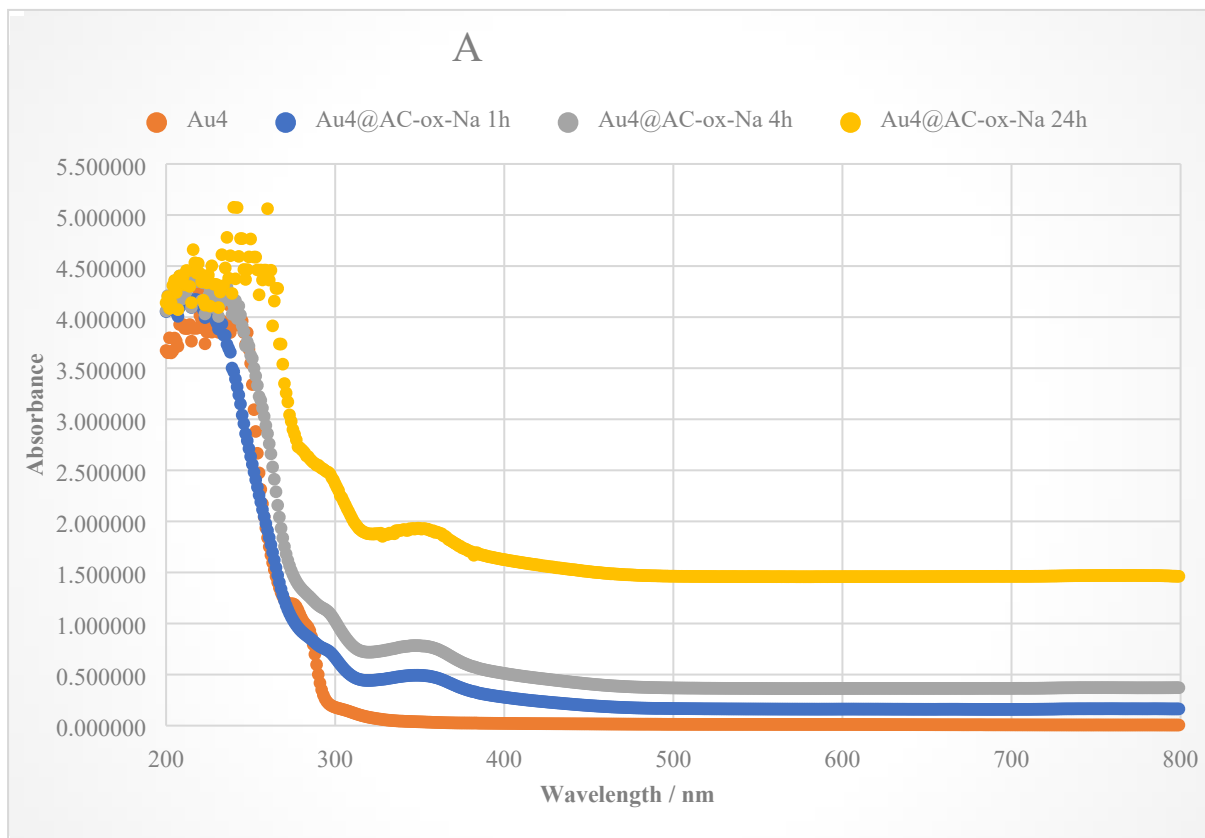


Figure S41. Heterogenization UV-Vis profiles throughout time of the supernatant from compound **4** on AC-ox-Na.

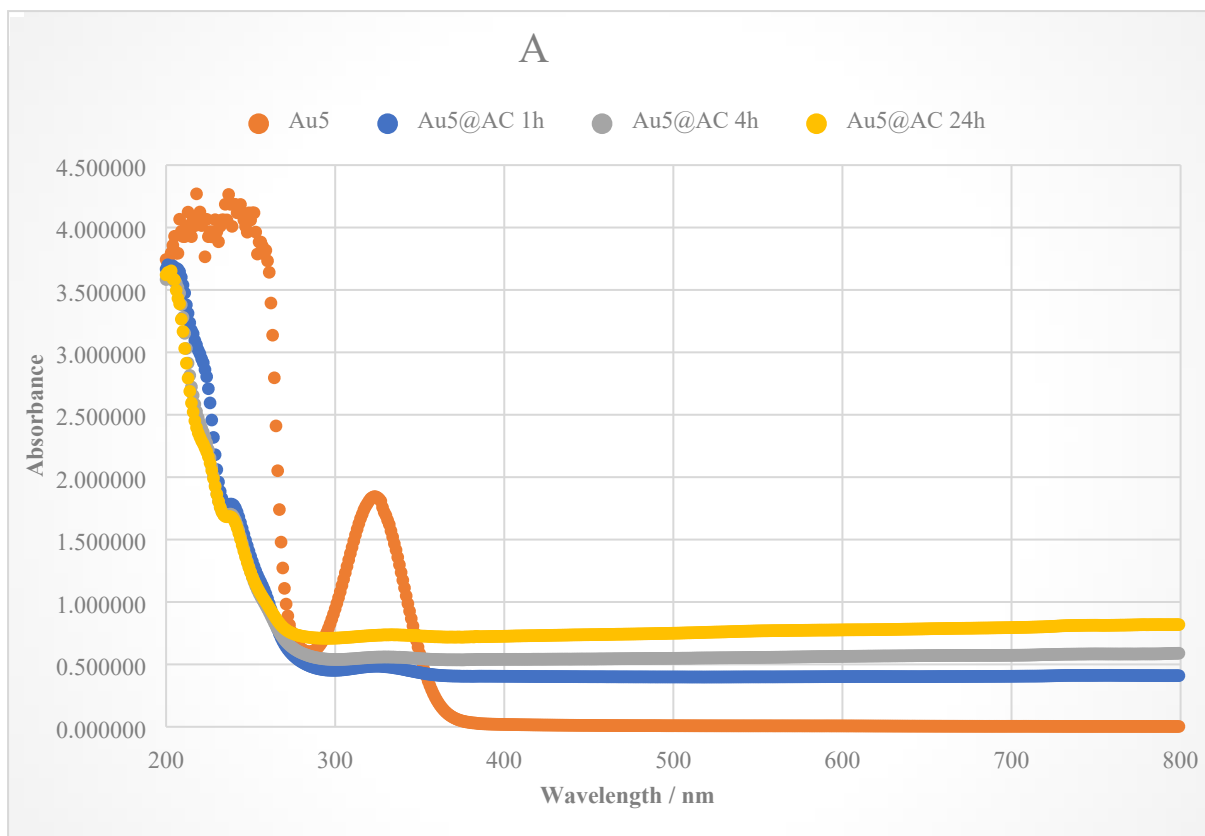


Figure S42. Heterogenization UV-Vis profiles throughout time of the supernatant from compound **5** on AC.

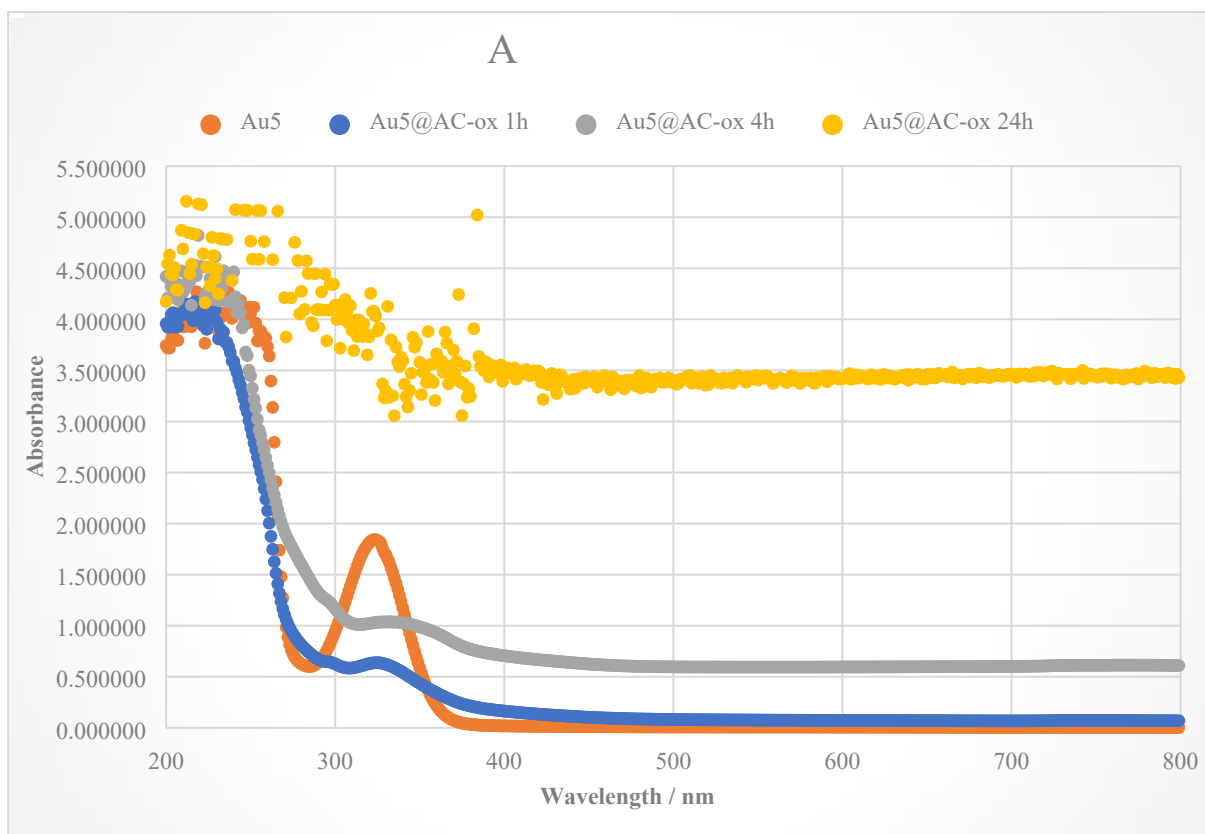


Figure S43. Heterogenization UV-Vis profiles throughout time of the supernatant from compound **5** on AC-ox.

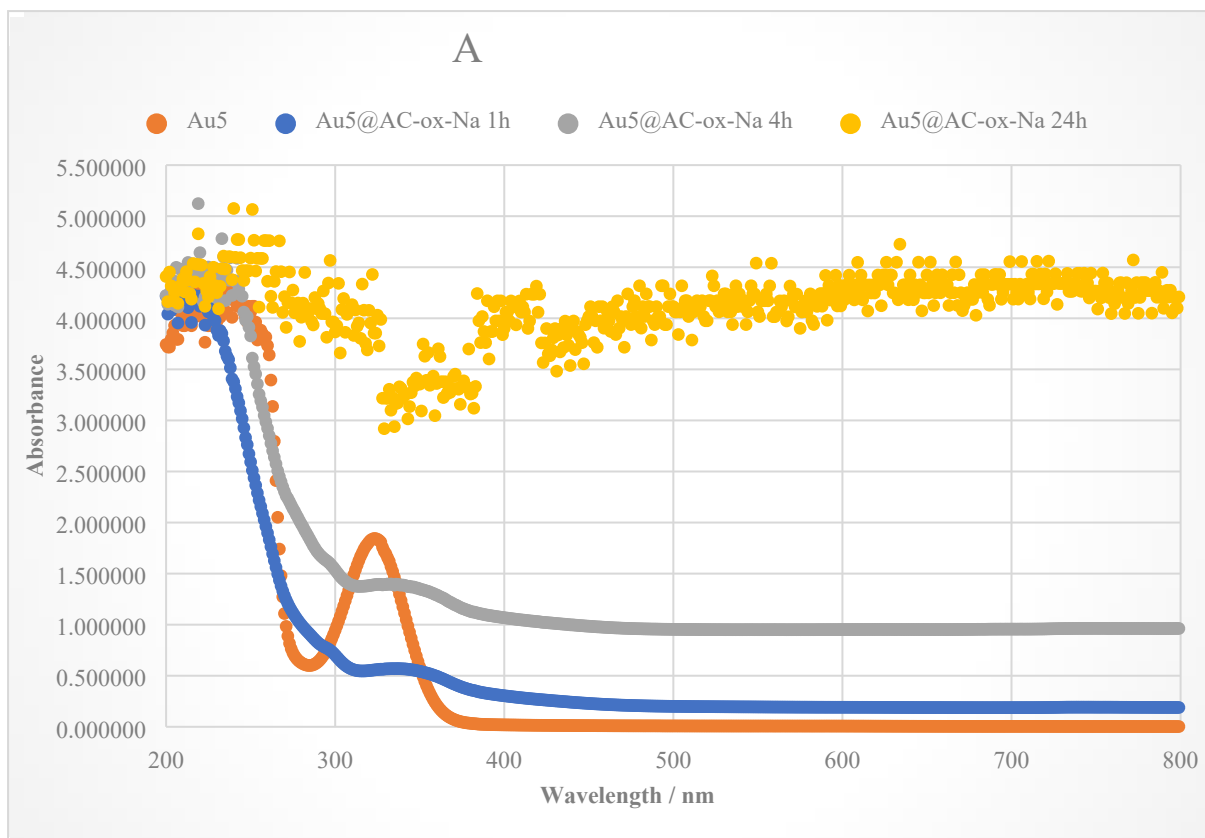


Figure S44. Heterogenization UV-Vis profiles throughout time of the supernatant from compound **5** on AC-ox-Na.

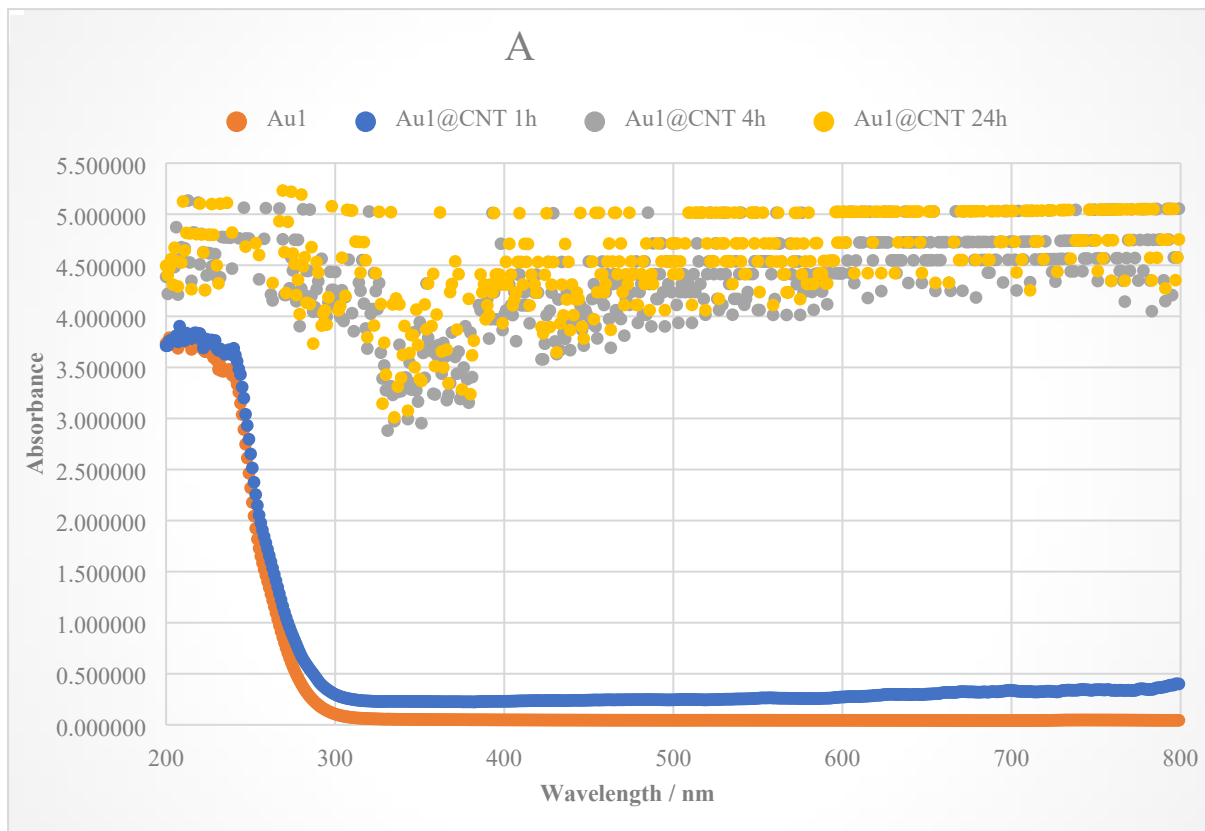


Figure S45. Heterogenization UV-Vis profiles throughout time of the supernatant from compound **1** on CNT.

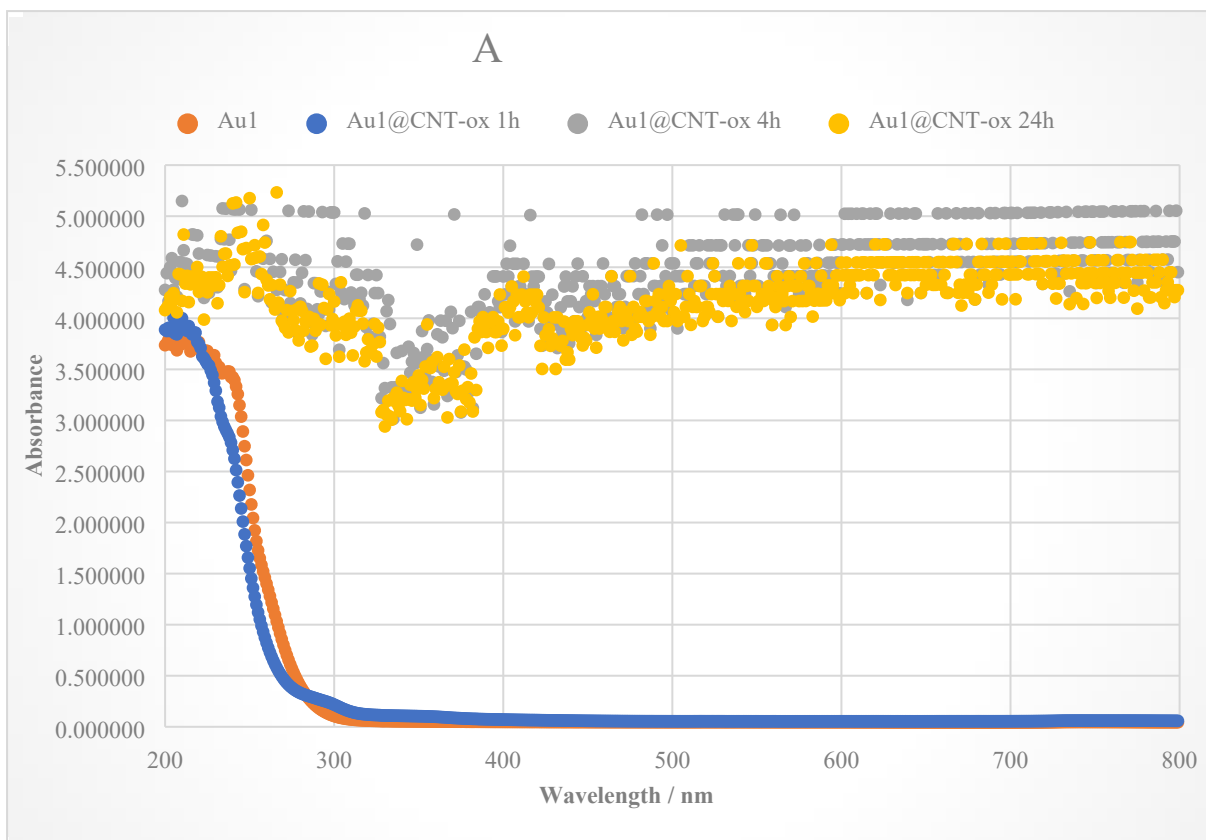


Figure S46. Heterogenization UV-Vis profiles throughout time of the supernatant from compound **1** on CNT-ox.

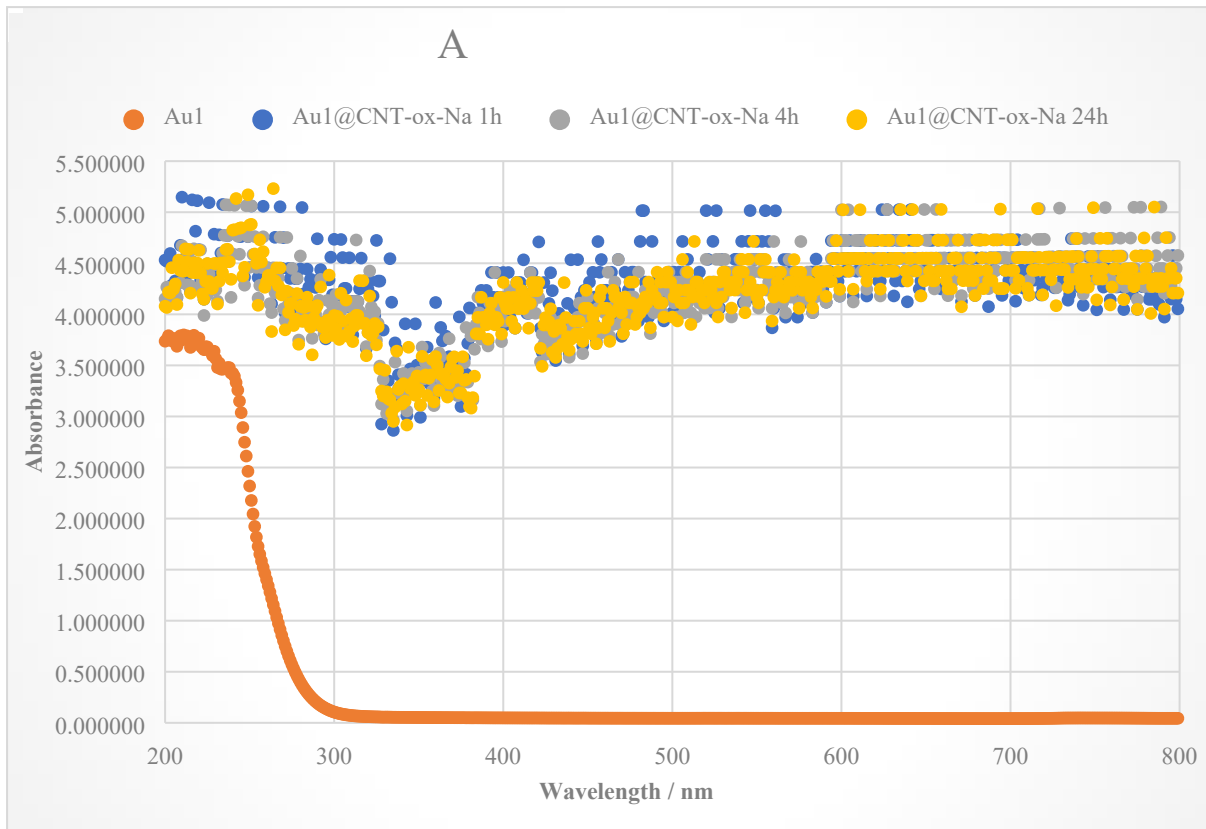


Figure S47. Heterogenization UV-Vis profiles throughout time of the supernatant from compound **1** on CNT-ox-Na.

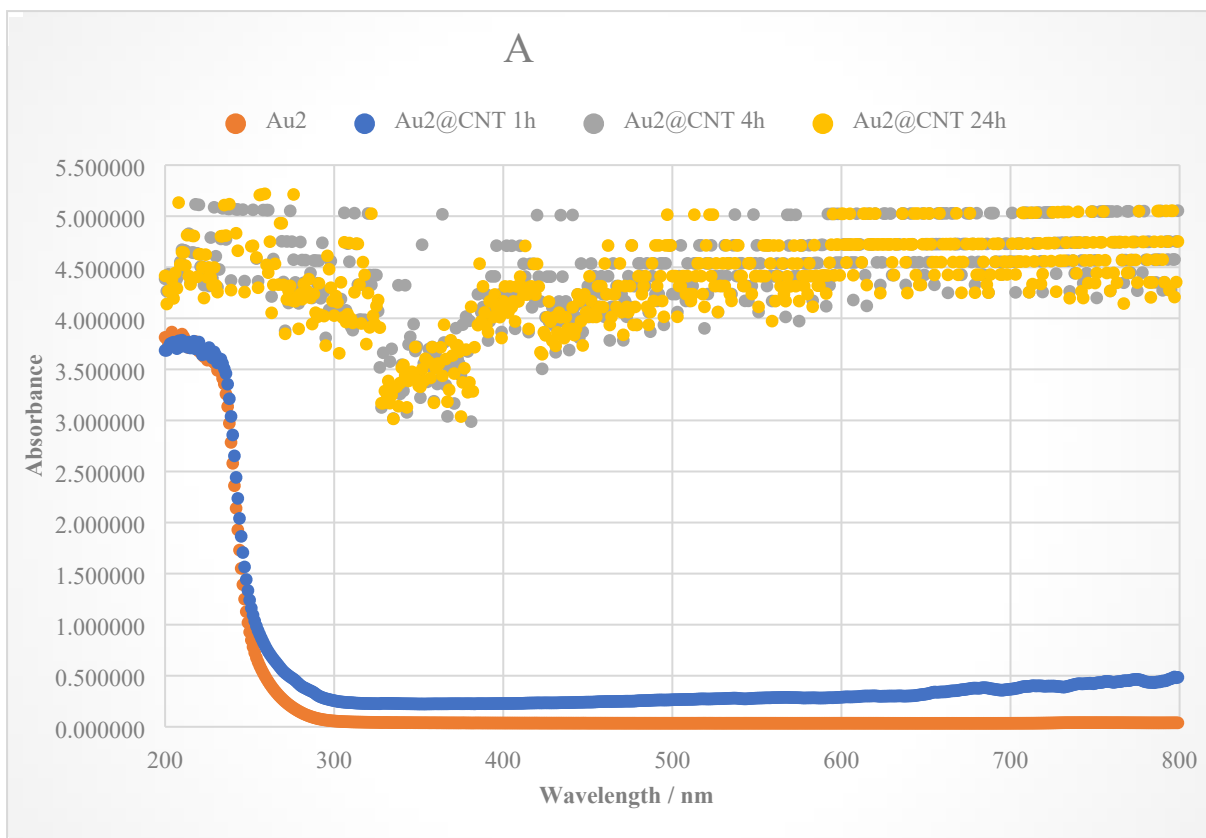


Figure S48. Heterogenization UV-Vis profiles throughout time of the supernatant from compound **2** on CNT.

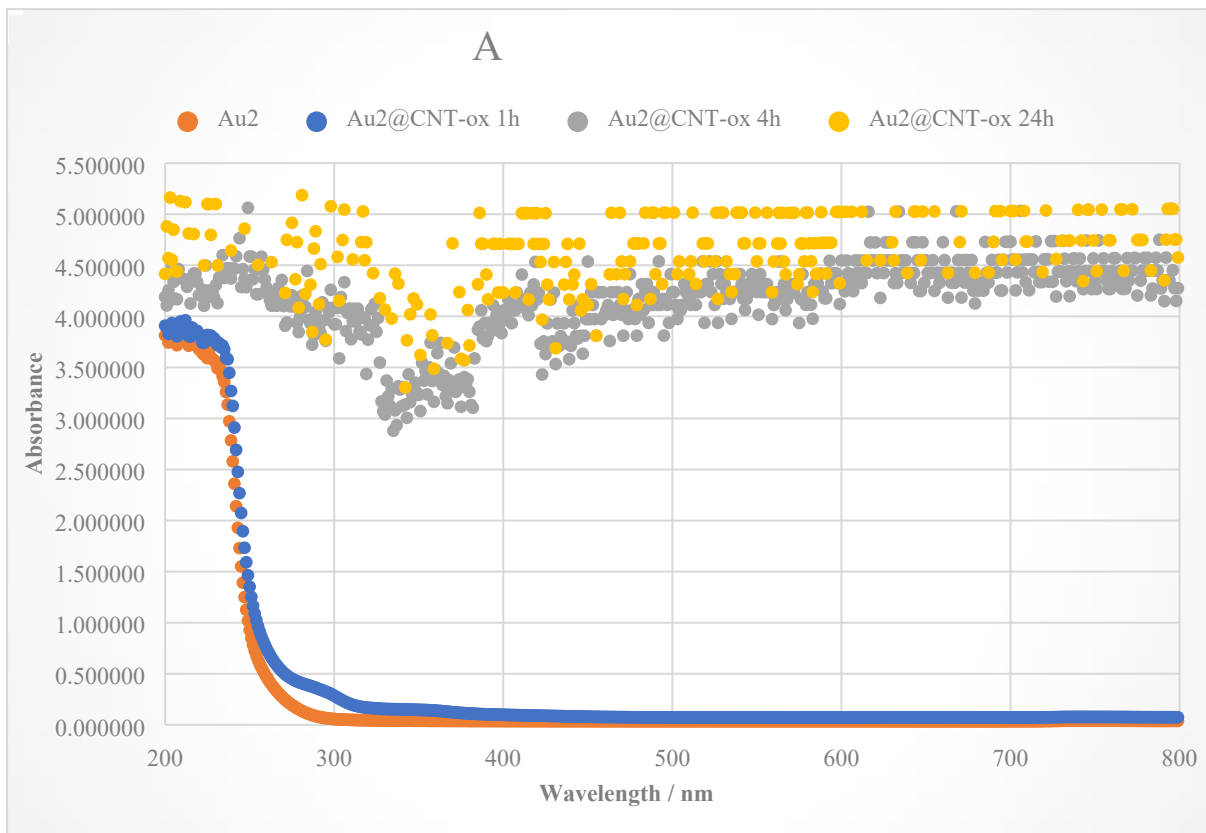


Figure S49. Heterogenization UV-Vis profiles throughout time of the supernatant from compound **2** on CNT-ox.

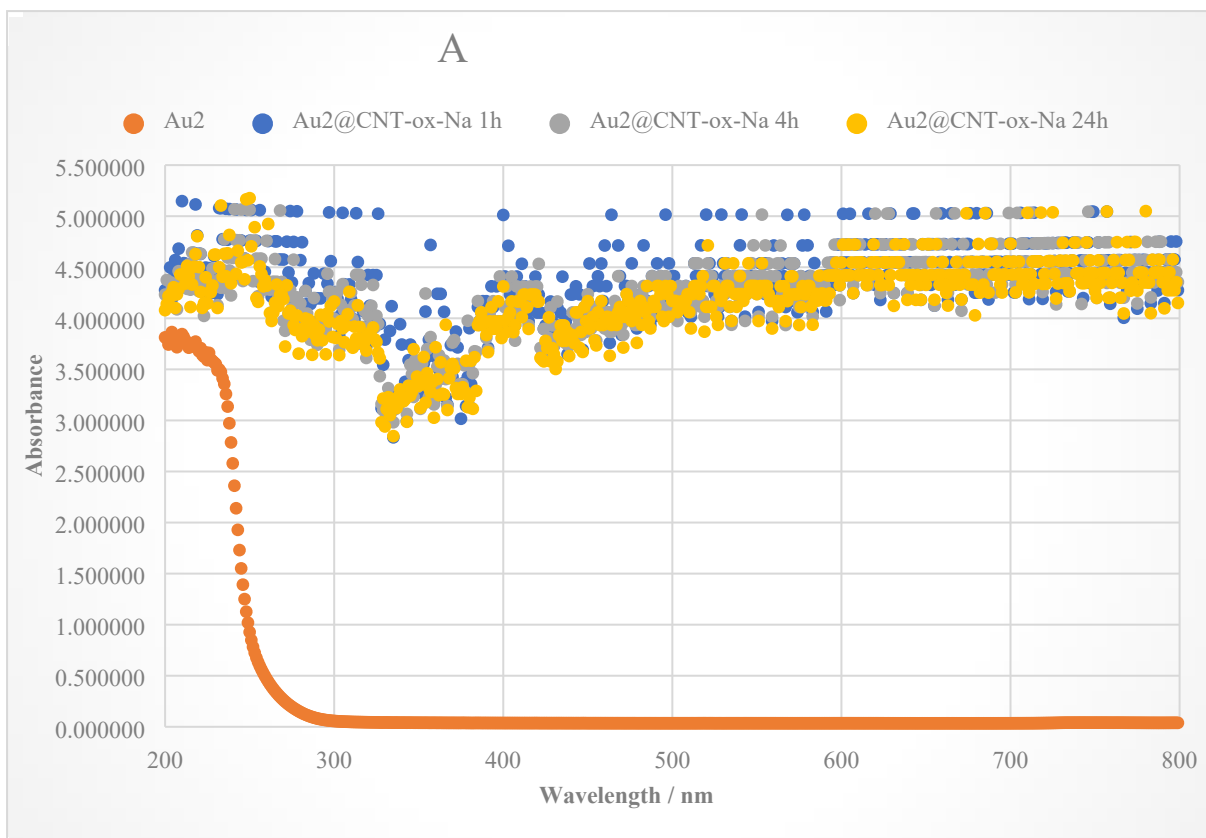


Figure S50. Heterogenization UV-Vis profiles throughout time of the supernatant from compound **2** on CNT-ox-Na.

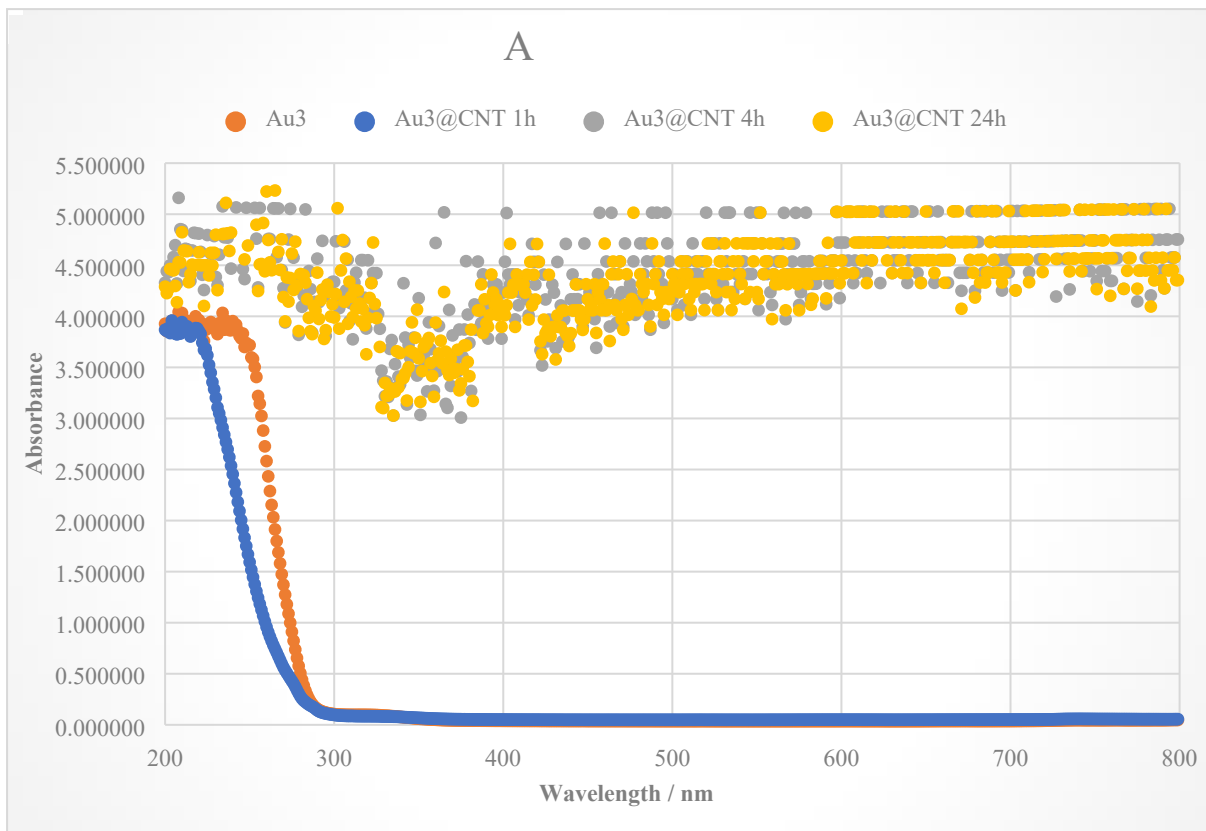


Figure S51. Heterogenization UV-Vis profiles throughout time of the supernatant from compound **3** on CNT.

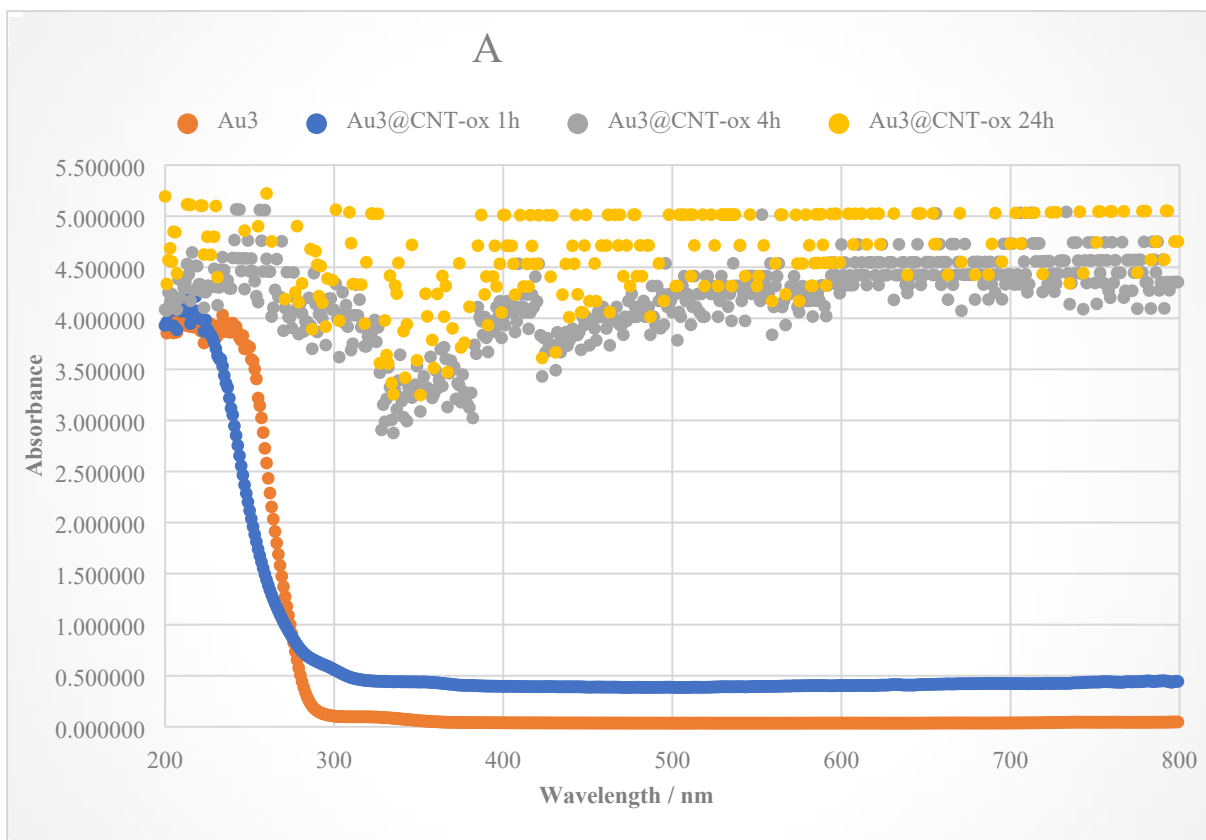


Figure S52. Heterogenization UV-Vis profiles throughout time of the supernatant from compound **3** on CNT-ox.

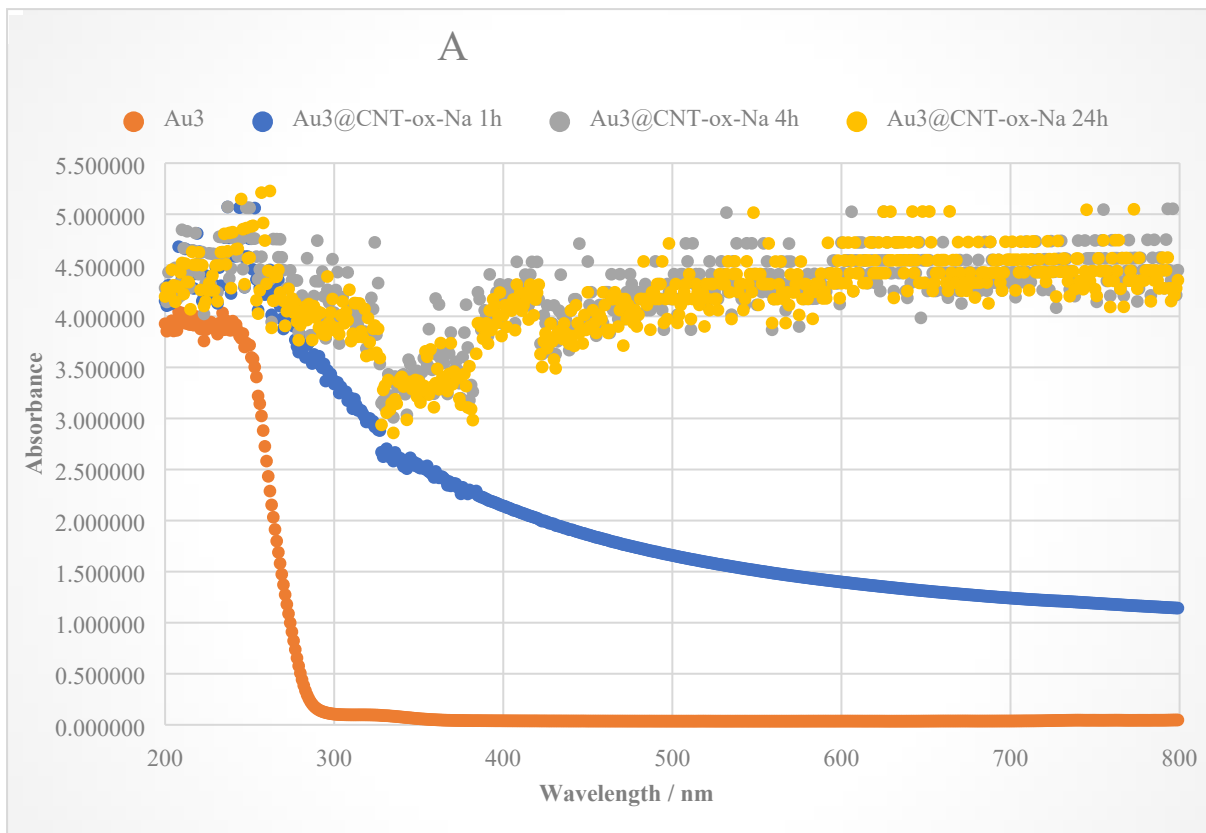


Figure S53. Heterogenization UV-Vis profiles throughout time of the supernatant from compound **3** on CNT-ox-Na.

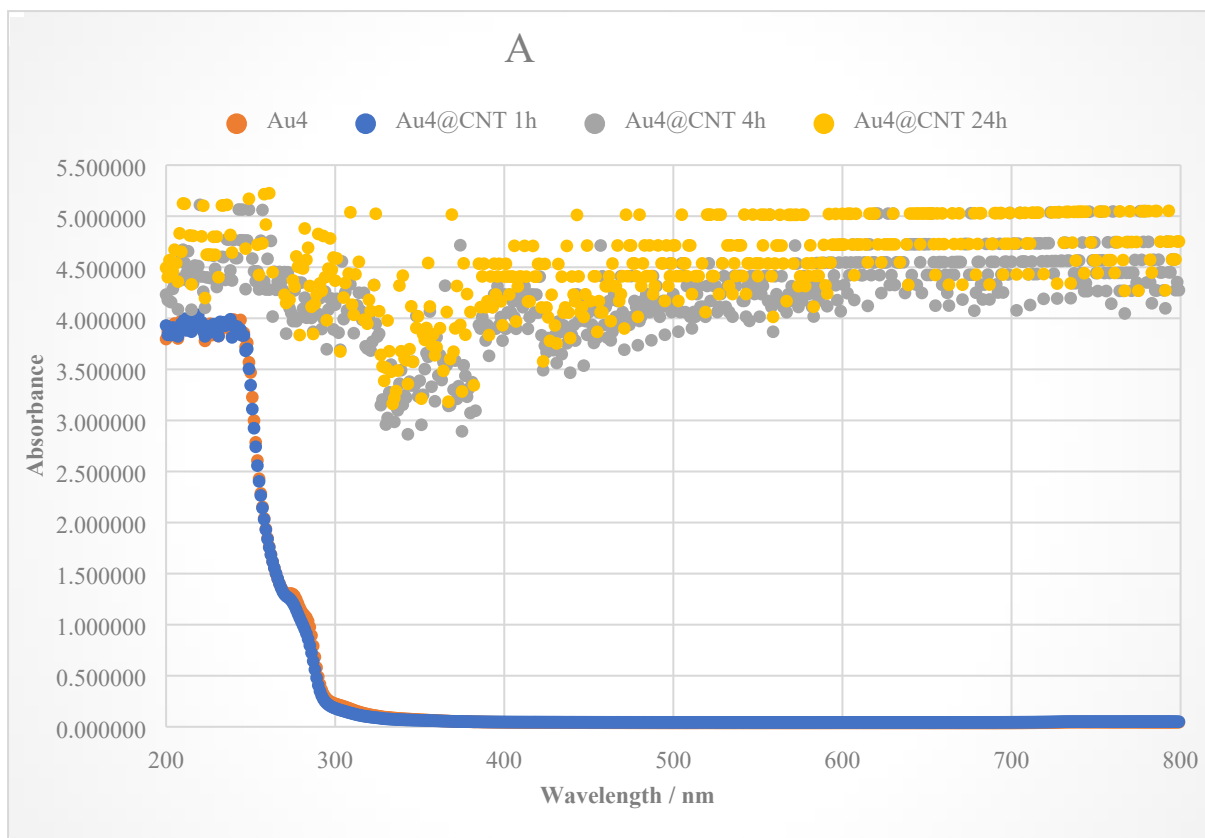


Figure S54. Heterogenization UV-Vis profiles throughout time of the supernatant from compound 4 on CNT.

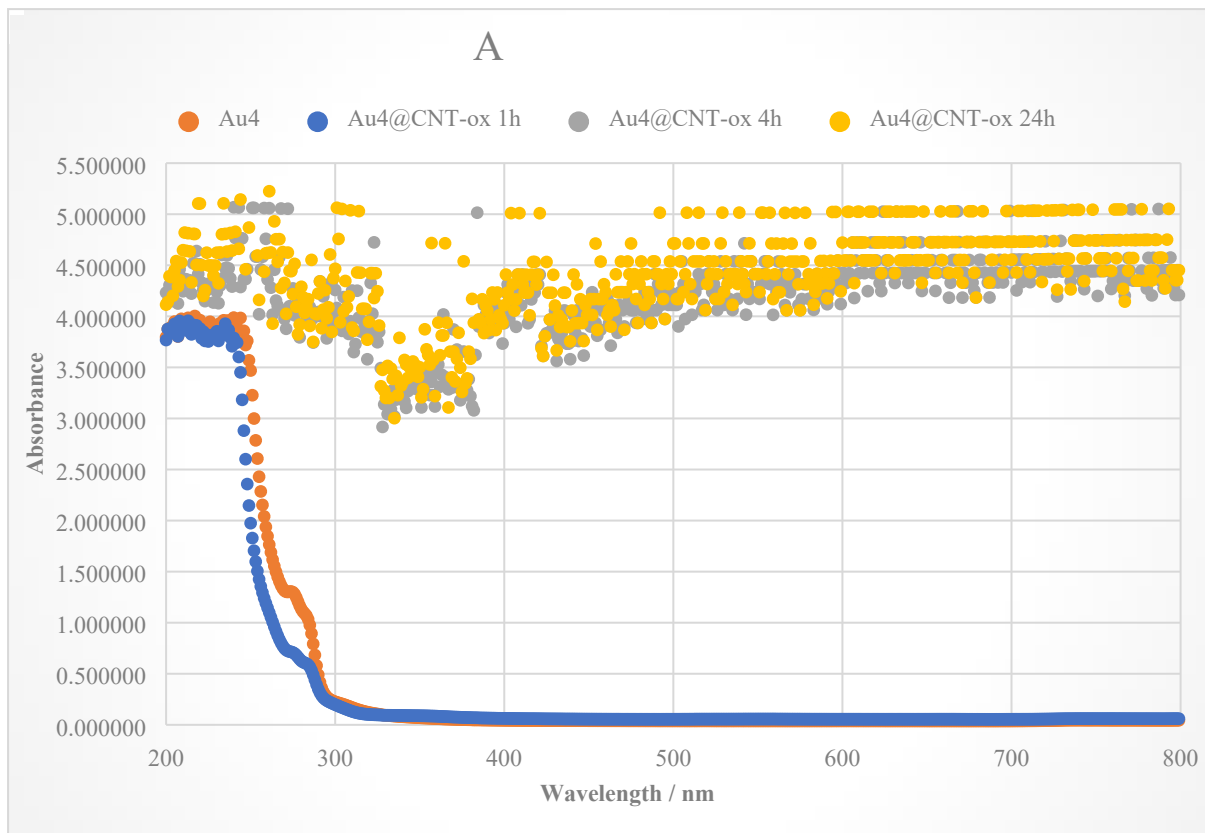


Figure S55. Heterogenization UV-Vis profiles throughout time of the supernatant from compound 4 on CNT-ox.

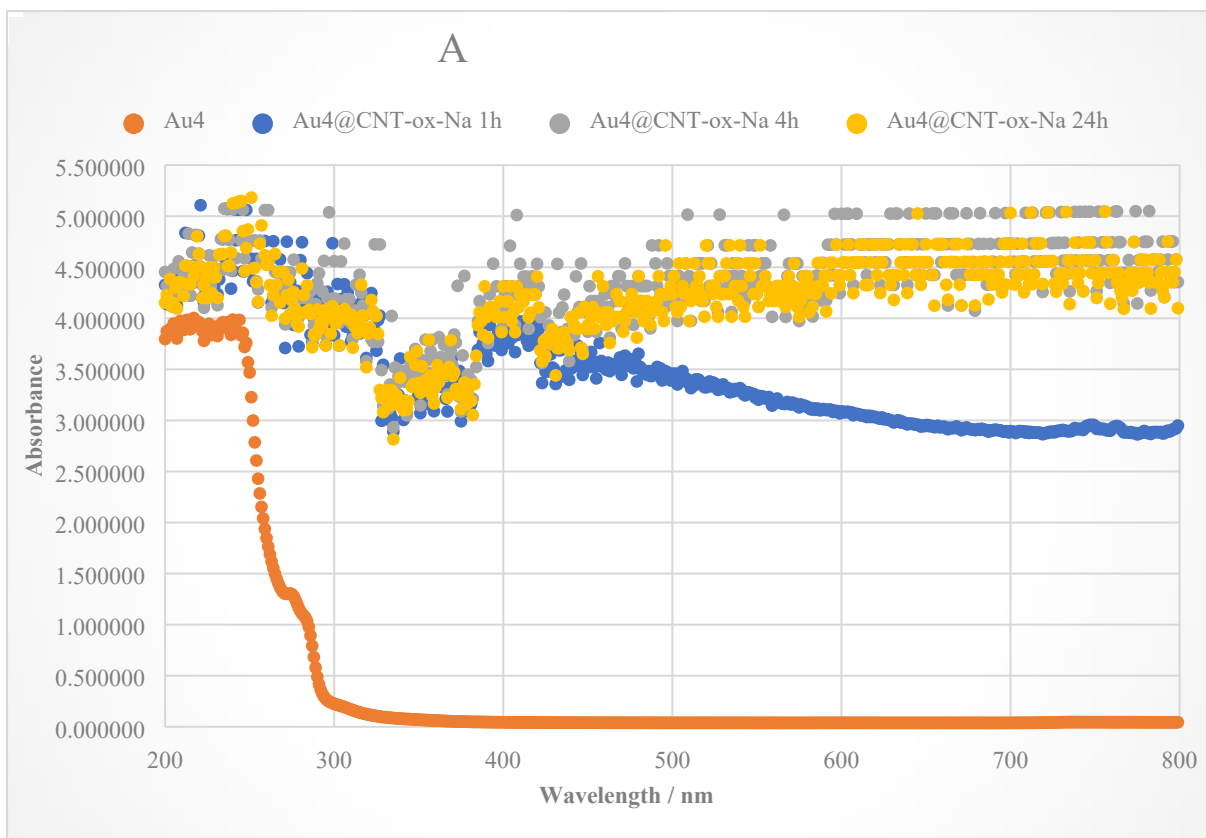


Figure S56. Heterogenization UV-Vis profiles throughout time of the supernatant from compound 4 on CNT-ox-Na.

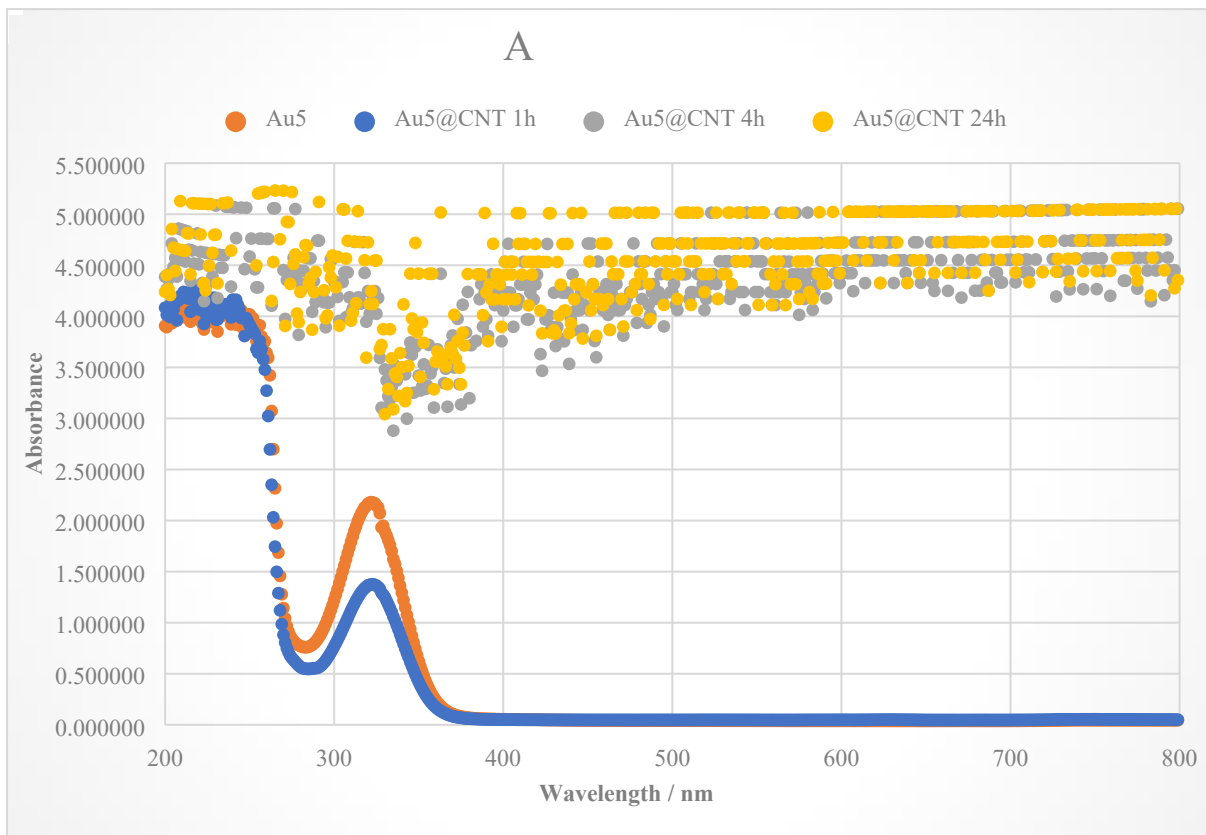


Figure S57. Heterogenization UV-Vis profiles throughout time of the supernatant from compound 5 on CNT.

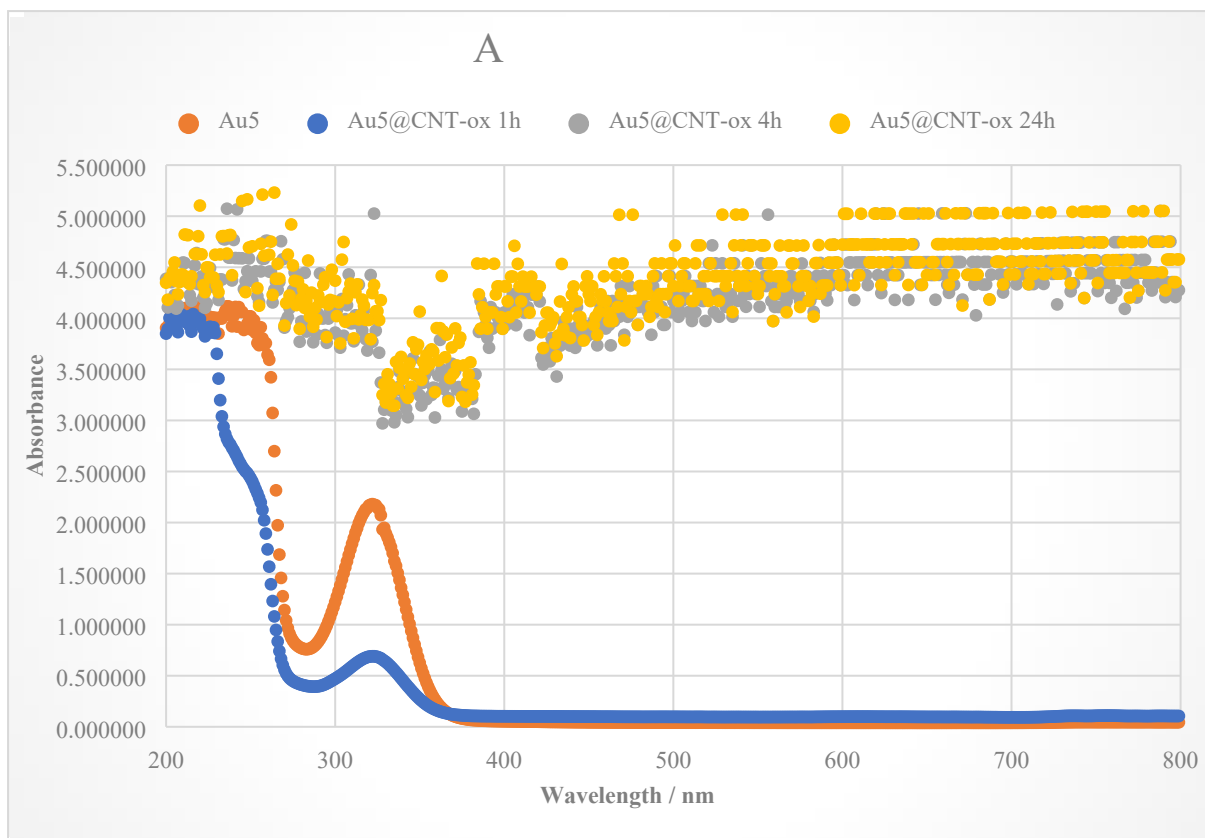


Figure S58. Heterogenization UV-Vis profiles throughout time of the supernatant from compound **5** on CNT-ox.

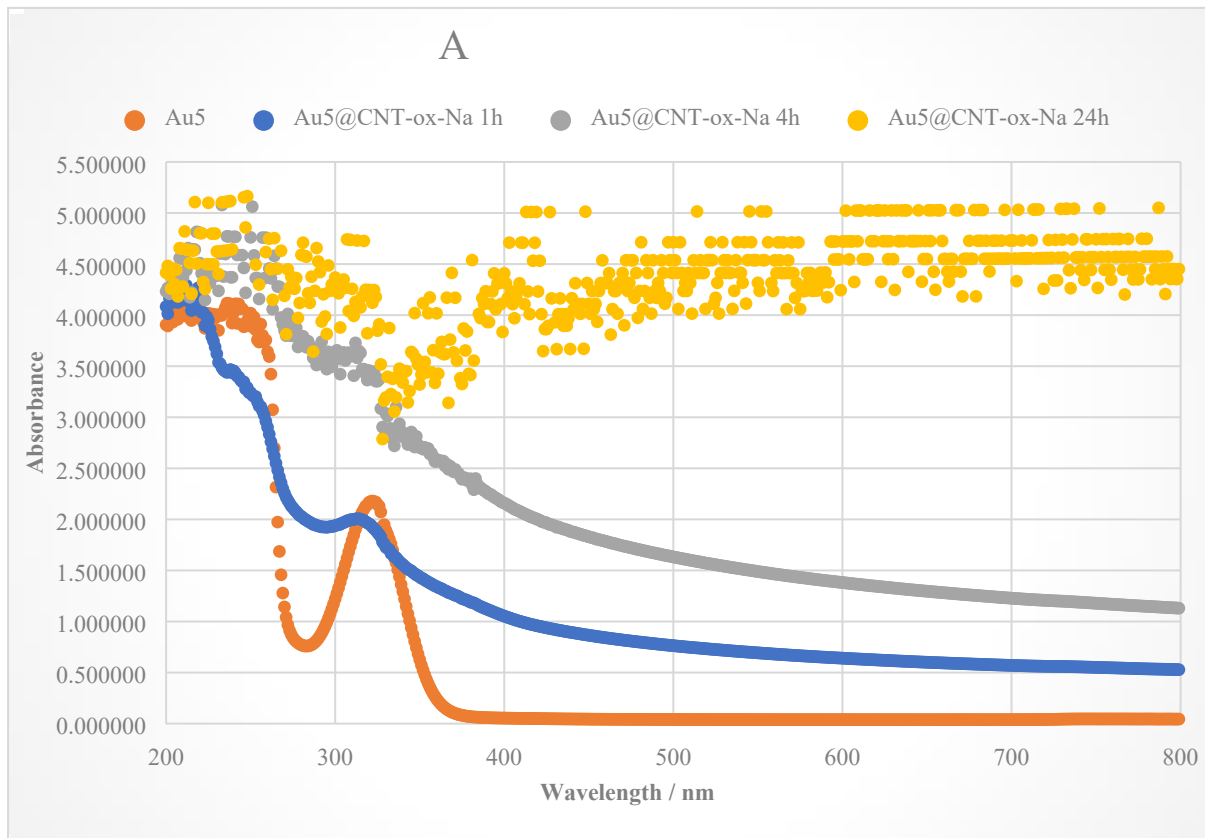


Figure S59. Heterogenization UV-Vis profiles throughout time of the supernatant from compound **5** on CNT-ox-Na.

Table S1. Characterization of carbon materials by adsorption of N₂ at -196 °C: surface area (S_{BET}), total pore volume (V_p), micropore volume (V_{mic}), average mesopore width (L), micropore volume (V_{micro}), and external area (S_{ext}) obtained by adsorption of N₂ at -196°C and amounts of desorbed CO and CO₂ determined by temperature programmed desorption. Adapted from our previous publication [63].

Sample	S _{BET} (m ² /g)	V _p (cm ³ /g)	L (nm)	V _{micro} (cm ³ /g)	S _{ext} (m ² /g)	CO (mmol/g)	CO ₂ (mmol/g)
AC	974	0.67	—	0.348	260	643	179
AC-ox	914	0.62	—	0.324	247	4930	2596
AC-ox-Na	610	0.35	—	0.251	80	5012	2883
CNT	257	2.89	—	~0	257	142	89
CNT-ox	400	1.89	—	~0	400	1475	729
CNT-ox-Na	350	1.45	—	~0	350	1079	838